Syntheses, Interconversions, and Structures of Mixed-Metal Rhodium–Osmium Clusters Derived from the Reaction of $(\mu\text{-H})_2Os_3(CO)_{10}$ with $(\eta^5\text{-}C_5Me_5)Rh(CO)_2$ and with $[(\eta^5\text{-}C_5Me_5)Rh(CO)]_2$

Deng-Yang Jan, Leh-Yeh Hsu, W.-L. Hsu, and Sheldon G. Shore*

Department of Chemistry, The Ohio State University, Columbus, Ohio 43210

Received July 7, 1986

The tetranuclear clusters $(\mu\text{-H})_2(\eta^5\text{-}C_5Me_5)RhOs_3(CO)_{10}$ (I) and $(\eta^5\text{-}C_5Me_5)_2Rh_2Os_2(CO)_8$ (III) are the principal cluster products obtained from reactions of $(\mu\text{-H})_2Os_3(CO)_{10}$ with $(\eta^5\text{-}C_5Me_5)Rh(CO)_2$ and with $[(\eta^5\text{-}C_5Me_5)Rh(CO)]_2$ in toluene at 90 °C in the absence of added hydrogen. In the presence of added H_2 at 1 atm the principal cluster products are $(\mu\text{-H})_4(\eta^5\text{-}C_5Me_5)RhOs_3(CO)_9$ (II) and $(\mu\text{-H}_2)(\eta^5\text{-}C_5Me_5)_2Rh_2Os_2(CO)_7$ (IV). Reactions are much more rapid when $[(\eta^5\text{-}C_5Me_5)Rh(CO)]_2$ is the starting material. Interconversions between clusters I and II and between III and IV have been observed. In the presence of H_2 at 1 atm and 90 °C in toluene, clusters I and II are converted to clusters III and IV, respectively. Reverse reactions occur in the presence of 1 atm of CO at 90 °C in toluene. The molecular structures of I–IV were determined through single-crystal X-ray diffraction studies. They have tetrahedral metal cores. Cluster III has an unusual structure in that each of the two Rh–Os–Rh trigonal faces are capped by a carbonyl group. For compound I: space group $P\bar{1}$, a = 10.473 (1) Å, b = 12.550 (1) Å, c = 9.598 (3) Å, α = 91.66 (2)°, β = 103.46 (2)°, γ = 84.54 (1)°, V = 1221.1 Å^3, Z = 2, mol wt = 1090.7, ρ_{calcd} = 2.968 g cm^{-3}, and μ_{calcd} = 162.9 cm^{-1} for Mo Kα; 4163 independent reflections $\geq 3\sigma(I)$; 4° $\leq 2\theta \leq$ 50°; final R_F = 3.4%, R_{wF} = 4.9%. For compound II: space group $P2_1/c$, a = 17.151 (5) Å, b = 18.360 (3) Å, c = 17.413 (4) Å, β = 114.85 (2)°, V = 4979.9 Å^3, Z = 8, mol wt = 1064.9, ρ_{calcd} = 2.845 g cm^{-3}, μ_{calcd} = 159.9 cm^{-1} for Mo Kα; 5580 independent reflections $\geq 3\sigma(I)$; 4° $\leq 2\theta \leq$ 50°; final R_F = 4.1%, R_{wF} = 5.5%. For compound III: space group $Ccca$, a = 15.966 (7) Å, b = 19.133 (5) Å, c = 20.701 (7) Å, V = 6323.8 Å^3, Z = 8, mol wt = 1080.9, ρ_{calcd} = 2.271 g cm^{-3}, μ_{calcd} = 90.8 cm^{-1} for Mo Kα; 2093 independent reflections $\geq 3\sigma(I)$; 4 $\leq 2\theta \leq$ 50°; final R_F = 5.3%, R_{wF} = 7.5%. For compound IV: space group $P2_1/c$, a = 10.923 (2) Å, b = 15.374 (2) Å, c = 17.869 (2) Å°, β = 96.39 (2)°, V = 2982.0 Å^3, Z = 4, mol wt = 1054.8, ρ_{calcd} = 2.350 g cm^{-3}, μ_{calcd} = 96.2 cm^{-1} for Mo Kα; 5641 independent reflections $\geq 3\sigma(I)$; 4° $\leq 2\theta \leq$ 50°; final R_F = 4.2%, R_{wF} = 5.4%. Spectroscopic data from clusters I through IV obtained in solution are consistent with the solid-state structure.

Introduction

A general route to triosmium-based mixed-metal clusters involves reactions of $(\mu\text{-H})_2Os_3(CO)_{10}$ with metal carbonyls under reaction conditions which cause formation of unsaturated metal carbonyl fragments generated under thermal[1-6] or photochemical[7] conditions.[8] While $(\mu\text{-H})_2Os_3(CO)_{10}$ has usually been employed as the starting material, it has also been generated in situ from $Os_3(CO)_{12}$ in the formation of the mixed-metal cluster in the presence of added H_2.[9,10] The effect of the presence or absence of added H_2 to the reaction system can determine the cluster products formed.[5,6,9,11] In the reaction involving $(\mu\text{-H})_2Os_3(CO)_{10}$ with the dimer $[Ni(\eta^5\text{-}C_5H_5)CO]_2$,[4,9] the presence of H_2 facilitates the reaction and is believed to assist in opening the dimer through the formation of an intermediate, reactive hydride.[9] The presence of added H_2 is required in order to obtain a reaction involving $(\mu\text{-H})_2Os_3(CO)_{10}$ and $[Mo(\eta^5\text{-}C_5H_5)(CO)_n]_2$ (n = 2, 3).[11] In this case also, reactive intermediate hydrides are believed to be formed through the reaction of H_2 with the dimeric molybdenum complex.

To date, the general approach described above has produced triosmium-based tetranuclear mixed-metal clusters when first-row transition-metal complexes are employed. However, reactions of $(\mu\text{-H})_2Os_3(CO)_{10}$ with carbonyl complexes of second-row transition metals gave other mixed-metal clusters in addition to triosmium-based tetranuclear species. Thus the H_2-initiated reaction of $[(\eta^5\text{-}C_5H_5)Mo(CO)_n]_2$ (n = 2, 3) with $(\mu\text{-H})_2Os_3(CO)_{10}$ in the presence of H_2 produces the pentanuclear cluster $(\mu\text{-H})_2(\eta^5\text{-}C_5H_5)_2Mo_2Os_3(CO)_{12}$ and two tetranuclear clusters $(\mu\text{-H})_3(\eta^5\text{-}C_5H_5)MoOs_3(CO)_{11}$ and $(\mu\text{-H})(\eta^5\text{-}C_5H_5)MoOs_3(CO)_{14}$.[11] The reaction of $(\mu\text{-H})_2Os_3(CO)_{10}$ with $(\eta^5\text{-}C_5H_5)Rh(CO)_2$ produces the trinuclear cluster $(\eta^5\text{-}C_5H_5)RhOs_2(CO)_9$ and the tetranuclear cluster $(\mu\text{-H})_2(\eta^5\text{-}C_5H_5)RhOs_3(CO)_{10}$[5] as the main products plus $(\mu\text{-H})_2(\eta^5\text{-}C_5H_5)_2Rh_2Os_2(CO)_7$.[12] From these earlier studies we found that the presence or absence of added H_2 in a re-

(1) Plotkin, J. S.; Alway, D. G. S.; Weisenberger, C. R.; Shore, S. G. *J. Am. Chem. Soc.* **1980**, *102*, 6156.
(2) Churchill, M. R.; Bueno, C.; Kennedy, S.; Bricker, J. C.; Plotkin, J. S.; Shore, S. G. *Inorg. Chem.* **1982**, *21*, 627.
(3) Shore, S. G.; Hsu, W.-L.; Weisenberger, C. R.; Caste, M. L.; Churchill, M. R.; Bueno, C. *Organometallics* **1982**, *1*, 1405.
(4) Churchill, M. R.; Bueno, C.; Hsu, W.-L.; Plotkin, J. S.; Shore, S. G. *Inorg. Chem.* **1982**, *21*, 1958.
(5) Hsu, L.-Y.; Hsu, W.-L.; Jan, D.-Y.; Marshall, A. G.; Shore, S. G. *Organometallics* **1984**, *3*, 591.
(6) Shore, S. G.; Hsu, W.-L.; Churchill, M. R.; Bueno, C. *J. Am. Chem. Soc.* **1983**, *105*, 655.
(7) Burkhardt, E. W.; Geoffroy, G. L. *J. Organomet. Chem.*, **1980**, *198*, 179.
(8) Stone and co-workers have developed a general method for the preparation of mixed-metal clusters from reactions of platinum metal–olefin complexes. Farrugia, L. J.; Howard, J. A. K.; Mitprachachon, P.; Spencer, J. L.; Stone, F. G. A.; Woodward, P. *J. Chem. Soc., Chem. Commun.* **1978**, *260*. See also ref 23.
(9) Castiglioni, M.; Sappa, E.; Valle, M.; Lanfranchi, M.; Tiripicchio, A. *J. Organomet. Chem.* **1983**, *241*, 99.
(10) Lavigne, G.; Papageorgiou, F.; Bergounhou, C.; Bonnet, J. J. *Inorg. Chem.* **1983**, *22*, 2485.
(11) Hsu, L.-Y.; Hsu, W.-L.; Jan, D.-Y.; Shore, S. G. *Organometallics* **1986**, *5*, 1041.
(12) Jan, D.-Y.; Hsu, L.-Y.; Hsu, W.-L.; Colombie, A.; Shore, S. G. *Abstracts of Papers*, 193rd National Meeting of the Americal Chemical Society, Annaheim, CA; American Chemical Society: Washington DC, 1986.

0276-7333/87/2306-0274$01.50/0

action system that contains $(\mu\text{-H})_2Os_3(CO)_{10}$ and a metal carbonyl can have a marked effect on the distribution of products formed.

In an effort to establish a more complete pattern of reactions between $(\mu\text{-H})_2Os_3(CO)_{10}$ and second-row transition-metal complexes and to expand the utility of this specific type of approach in the syntheses of mixed-metal clusters, the reaction of $(\mu\text{-H})_2Os_3(CO)_{10}$ with $(\eta^5\text{-}C_5Me_5)Rh(CO)_2$ and with $[(\eta^5\text{-}C_5Me_5)Rh(CO)]_2$ in the presence and absence of added H_2 has been studied in the present investigation. We report here syntheses, interconversions, and X-ray structures of $(\mu\text{-H})_2(\eta^5\text{-}C_5Me_5)RhOs_3(CO)_{10}$ (I), $(\mu\text{-H})_4(\eta^5\text{-}C_5Me_5)RhOs_3(CO)_9$ (II), $(\eta^5\text{-}C_5Me_5)Rh_2Os_2(CO)_8$ (III), and $(\mu\text{-H})_2(\eta^5\text{-}C_5Me_5)_2Rh_2Os_2(CO)_7$ (IV). Additionally, these structures are compared with structures of related clusters containing other metals.

Experimental Section

Chemicals and Solvents. Rhodium trichloride trihydrate was purchased for Strem Chemicals, Inc., and used as received. Pentamethylcyclopentadiene was obtained from Aldrich Chemical Co. and used as received. Prepurified hydrogen was obtained from AGA, Inc., and used without further purification. Carbon monoxide, 99.9%, was purchased from Matheson Scientific Products. It was passed through a −196 °C trap to remove H_2O and CO_2 prior to use. Carbon monoxide, 99% ^{13}C enriched, was obtained from Monsanto Co. (Mound Laboratory) and used as received. The starting materials $(\mu\text{-H})_2Os(CO)_{10}$,[13] and $[(\eta^5\text{-}C_5Me_5)Rh(CO)]_2$[14] were prepared according to published methods while $(\eta^5\text{-}C_5Me_5)Rh(CO)_2$ was prepared by following the method employed to synthesize the cyclopentadienyl analogue.[15] Chemical analyses were performed by Schwarzkopf Microanalytical Laboratories.

Infrared and NMR Spectra. Infrared spectra of solutions in matched cells were recorded on a Matteson Cygnus-25 FT spectrometer. Proton and carbon-13 NMR spectra were obtained on a Bruker WM-300 spectrometer at 300.13 and 75.47 MHz, respectively. Chemical shifts are referred to $Si(CH_3)_4$ (^1H, δ = 0.00; ^{13}C, δ = 0.00).

Preparation of $(\mu\text{-H})_2(\eta^5\text{-}C_5Me_5)RhOs_3(CO)_{10}$, $(\eta^5\text{-}C_5Me_5)_2Rh_2Os_2(CO)_8$, and $(\mu\text{-H})_2(\eta^5\text{-}C_5Me_5)_2Rh_2Os_2(CO)_7$ in the Absence of Added H_2. Both $(\mu\text{-H})_2Os_3(CO)_{10}$ (61.4 mg, 0.072 mmol) and $(\eta^5\text{-}C_5Me_5)Rh(CO)_2$ (43.5 mg, 0.148 mmol) were weighed into a 50-mL round-bottomed flask, which was equipped with a Kontes Teflon stopcock. This flask was then placed on a vacuum line and evacuated, the toluene (7.0 mL) was then condensed into it. The flask under vacuum was then heated at 90 °C for 103 h. During this period, the CO generated was pumped away once every 24 h. The volatile components were removed from the reaction mixture, leaving a dark brown residue. This residue was then dissolved in a minimum amount of CH_2Cl_2 and chromatographed on a preparative thin-layer plate (2-mm silica gel). Elution with 1:4 benzene/hexane yielded three bands. In the order of decreasing R_f value, they are greenish brown, reddish brown, and dark brown.

The greenish brown band was identified as $(\mu\text{-H})_2(\eta^5\text{-}C_5Me_5)RhOs_3(CO)_{10}$ (9.6 mg, 12% yield based on $(\mu\text{-H})_2Os_3(CO)_{10}$) from a single-crystal X-ray diffraction analysis. Single crystals of $(\mu\text{-H})_2(\eta^5\text{-}C_5Me_5)RhOs_3(CO)_{10}$ were grown from CH_2Cl_2/hexane at −15 °C. Its FT/ICR mass spectrum was obtained with a Nicolet FT/MS-100 Fourier transform ion cyclotron mass spectrometer equipped with a 2.0 magnet and a 1-in. cubic cell and showed a parent ion peak which corresponds to the molecular formula $^1H_{17}{}^{12}C_{20}{}^{16}O_{10}{}^{103}Rh^{192}Os_3$: m/e (obsd) 1096, m/e (calcd) 1096. The loss of each of the 10 carbonyls was visible in a single spectrum. ^1H NMR (THF-d_8, −90 °C): δ −1.89 (15 H, s), −16.53 (1 H, s), −20.08 (1 H, s). IR (ν_{CO}, cyclohexane) 1792 (m), 1962 (w), 1969 (w), 2002 (s), 2041 (s), 2064 (s), 2084 (m) cm^{-1}. Anal. Calcd for $C_{20}H_{17}O_{10}Os_3Rh$: C, 22.02; H, 1.57. Found: C, 22.27; H, 1.60.

The reddish brown band was identified as $(\mu\text{-H})_2(\eta^5\text{-}C_5Me_5)_2Rh_2Os_2(CO)_7$ (8.2 mg, 7.2% yield based on $(\mu\text{-H})_2Os_3(CO)_{10}$) from a single-crystal X-ray structure determination. Single crystals of $(\mu\text{-H})_2(\eta^5\text{-}C_5Me_5)_2Rh_2Os_2(CO)_7$ were grown from CH_2Cl_2/hexane at −15 °C. ^1H NMR (CD_2Cl_2, −90 °C): δ 1.94 (15 H, s), 1.92 (15 H, s), −14.57 (1 H, s), −18.80 (1 H, d, J_{Rh-H} = 26 Hz). ^{13}C NMR (CH_2Cl_2, −90 °C): δ 238.76 (1 C, t, J_{Rh-C} = 44 Hz), 190.98 (1 C, s), 185.23 (1 C, s), 182.72 (1 C, s), 176.94 (1 C, s), 173.62 (1 C, d, J_{C-H} = 9.3 Hz), 172.86 (1 C, s). IR (ν_{CO}, cyclohexane): 1796 (m), 1941 (m), 1949 (m), 1980 (s), 1989 (m), 2024 (s), 2061 (s) cm^{-1}. Anal. Calcd for $C_{27}H_{32}O_7Os_3Rh$: C, 30.74; H, 3.06. Found: C, 30.73; H, 2.93.

The dark brown band was identified as $(\eta^5\text{-}C_5Me_5)_2Rh_2Os_2(CO)_8$ (46.7 mg, 40% yield based on $(\mu\text{-H})_2Os_3(CO)_{10}$) from a single-crystal X-ray structure determination. Single crystals were grown from CH_2Cl_2/hexane at −15 °C. ^1H NMR (CD_2Cl_2, 27 °C): δ 1.70 (30 H, s). ^{13}C NMR (CD_2Cl_2, −90 °C): δ 240.18 (2 C, t, J_{Rh-C} = 34 Hz), 186.18 (6 C, s). IR (ν_{CO}, cyclohexane): 1674 (w), 1698 (w), 1956 (m), 1973 (s), 2018 (s), 2046 (s) cm^{-1}. Anal. Calcd for $C_{28}H_{30}O_8Os_2Rh_2$: C, 31.11; H, 2.80. Found: C, 30.39; H, 2.67.

This reaction was repeated by using the unsaturated dimer $[(\eta^5\text{-}C_5Me_5)Rh(CO)]_2$ (38.9, mg, 0.073 mmol) and $(\mu\text{-H})_2Os_3(CO)_{10}$ (60.5 mg, 0.071 mmol). The solvent and temperature were the same as given above. However, only 1 h was required for the reaction to go to completion. Yields of products: $(\mu\text{-H})_2(\eta^5\text{-}C_5Me_5)RhOs_3(CO)_{10}$, 5.4 mg (7%); $(\mu\text{-H})_2(\eta^5\text{-}C_5Me_5)_2Rh_2Os_2(CO)_7$, 7.9 mg (7%); $(\eta^5\text{-}C_5Me_5)_2Rh_2Os_2(CO)_8$, 48.3 mg (42%).

Preparation of $(\mu\text{-H})_4(\eta^5\text{-}C_5Me_5)RhOs_3(CO)_9$ and $(\mu\text{-H})_2(\eta^5\text{-}C_5Me_5)_2Rh_2Os_2(CO)_7$ in the Presence of Added H_2. Both $(\mu\text{-H})_2Os_3(CO)_{10}$ (0.072 mmol) and $(\eta^5\text{-}C_5Me_5)Rh(CO)_2$ (0.150 mmol) were weighed into a 50-mL three-necked flask connected to a reflux condenser which was then flushed with H_2 for 20 min, and freshly distilled toluene (10 mL) was then syringed into the reaction vessel. The hydrogen flow was adjusted to slowly bubble through the solution, and the reaction flask was then heated to 90 °C for 96 h. The same procedure as described above was employed to work up the reaction products. In order of decreasing R_f value the products were a reddish orange band and a reddish brown band. This second band was identified as $(\mu\text{-H})_2(\eta^5\text{-}C_5Me_5)_2Rh_2Os_2(CO)_7$ on the basis of its IR and ^1H NMR spectra compared with the spectra cited above. This product was isolated in 41.0-mg quantity (36% yield based on $(\mu\text{-H})_2Os_3(CO)_{10}$).

The reddish orange band was identified as $(\mu\text{-H})_4(\eta^5\text{-}C_5Me_5)RhOs_3(CO)_9$ (27.6 mg, 36% based on $(\mu\text{-H})_2Os_3(CO)_{10}$) from a single-crystal X-ray structure determination. Single crystals were grown from CH_2Cl_2/hexane at −15 °C. ^1H NMR ($CDCl_3$, −60 °C): δ 1.94 (15 H, s), −15.17 (2 H, d, J_{Rh-H} = 18 Hz), −19.68 (2 H, s). IR (ν_{CO}, cyclohexane): 1984 (s), 1992 (m (sh)), 2006 (s), 2047 (s), 2053 (s), 2083 (m) cm^{-1}. Anal. Calcd for $C_{19}H_{19}O_9Os_3Rh$: C, 21.43; H, 1.80. Found: C, 21.19; H, 1.76.

The reaction was repeated by using the unsaturated dimer $[(\eta^5\text{-}C_5Me_5)Rh(CO)]_2$ (38.3 mg, 0.073 mmol) and $(\mu\text{-H})_2Os_3(CO)_{10}$ (59.7 mg, 0.070 mmol). Reaction conditions were the same as given above. However, only 1 h was required for the reaction to go to completion. Yields of products: $(\mu\text{-H})_4(\eta^5\text{-}C_5Me_5)RhOs_3(CO)_9$, 13.4 mg (18%); $(\mu\text{-H})_2(\eta^5\text{-}C_5Me_5)_2Rh_2Os_2(CO)_7$, 27.7 mg (25%); $(\mu\text{-H})_2(\eta^5\text{-}C_5Me_5)RhOs_3(CO)_{10}$, 3.1 mg (4%).

Interconversion of $(\mu\text{-H})_2(\eta^5\text{-}C_5Me_5)RhOs_3(CO)_{10}$ and $(\mu\text{-H})_4(\eta^5\text{-}C_5Me_5)RhOs_3(CO)_9$. A toluene solution (4.5 mL) of $(\mu\text{-H})_2(\eta^5\text{-}C_5Me_5)RhOs_3(CO)_{10}$ (11.3 mg, 0.0103 mmol) in a 50-mL round-bottomed flask was frozen at −196 °C and evacuated. The reaction vessel was warmed to −78 °C, and H_2 (685 torr) was then added to the system. The reaction was maintained at 90 °C and monitored by both thin-layer chromatography and infrared spectroscopy. $(\mu\text{-H})_2(\eta^5\text{-}C_5Me_5)RhOs_3(CO)_9$ formed slowly under the reaction conditions and became the major product (70% yield) after a period of 7 days. The reverse conversion of $(\mu\text{-H})_4(\eta^5\text{-}C_5Me_5)RhOs_3(CO)_9$ to $(\mu\text{-H})_2(\eta^e\text{-}C_5Me_5)RhOs_3(CO)_{10}$, using similar amounts of reactants as in the forward reaction, was conducted at 90 °C with CO (685 torr) present over the reaction solution. After 7 days $(\mu\text{-H})_2(\eta^5\text{-}C_5Me_5)RhOs_3(CO)_{10}$ was the major product. Some decomposition occurred.

Interconversion of $(\eta^5\text{-}C_5Me_5)_2Rh_2Os_2(CO)_8$ and $(\mu\text{-H})_2(\eta^5\text{-}C_5Me_5)_2Rh_2Os_2(CO)_7$. A toluene solution (3.5 mL) of III (11.9

(13) Knox, S. A. R.; Koepke, J. W.; Andrews, M. A.; Kaesz, H. D. *J. Am. Chem. Soc.* **1975**, *97*, 3942.
(14) Aldridge, M. L.; Green, M.; Howard, J. A. K.; Pain, G. N.; Porter, S. J.; Stone, F. G. A. *J. Chem. Soc., Dalton Trans.* **1982**, 1333.
(15) Blackmore, T.; Bruce, M. I.; Stone, F. G. A. *J. Chem. Soc. A* **1968**, 2158.

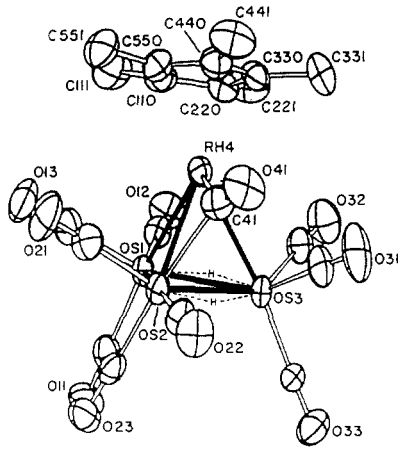

Figure 1. Molecular structure of $(\mu\text{-H})_2(\eta^5\text{-}C_5Me_5)RhOs_3(CO)_{10}$ (50% probability ellipsoids).

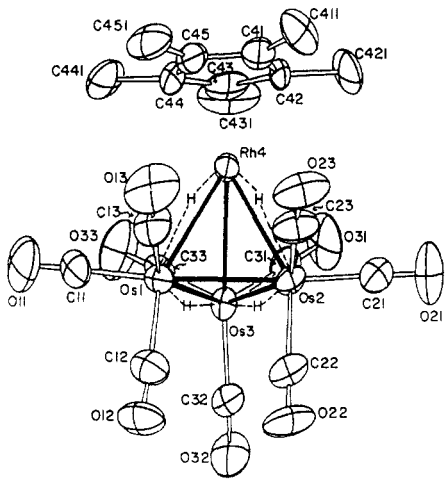

Figure 2. Molecular structure of $(\mu\text{-H})_4(\eta^5\text{-}C_5Me_5)RhOs_3(CO)_9$ (50% probability ellipsoids).

mg, 0.011 mmol) was frozen at −196 °C and then evacuated. H_2 (685 torr) was then transferred to the reaction vessel at −78 °C. The reaction was kept at 90 °C and monitored by both thin-layer chromatography and infrared spectroscopy. The conversion passed the midpoint after a period of 4 days and was complete after 7 days without observable decomposition. The reverse reaction, using similar amounts of reactants as in the forward reaction, conducted at 90 °C with CO (685 torr) present over the solution was complete in a period of 36 h with negligible fragmentation of the cluster.

X-ray Structure Determinations. For X-ray examination and data collection, each crystal was mounted at the tip of a thin glass fiber. All X-ray data were collected on a Enraf-Nonius CAD-4 diffractometer with graphite-monochromated Mo Kα radiation, and all the crystallographic computations were carried out on a PDP 11/44 computer using SDP (Structure Determination Package).[16] Table I gives crystal data.

For each crystal, unit cell parameters were obtained by least-squares refinement of the angular setting from 24 reflections, well distributed in reciprocal space and lying in a 2θ range of 24°–30°. Intensity data were collected in the ω–2θ scan mode. Six standard reflections were monitored and showed no significant decay. The data were corrected for Lorentz and polarization effects. Intensities were also corrected for absorption by using an empirical method based on the crystal orientation and measured ψ scans.

All structures were solved by a combination of the direct method (MULTAN 11/82) and the difference Fourier technique, and they were refined by full-matrix least squares. Analytical

(16) SDP (developed by B. A. Frenz and Associated, Inc., College Station, TX 77840) was used to process X-ray data, apply corrections, solve and refine the structures, produce drawings, and print tables.

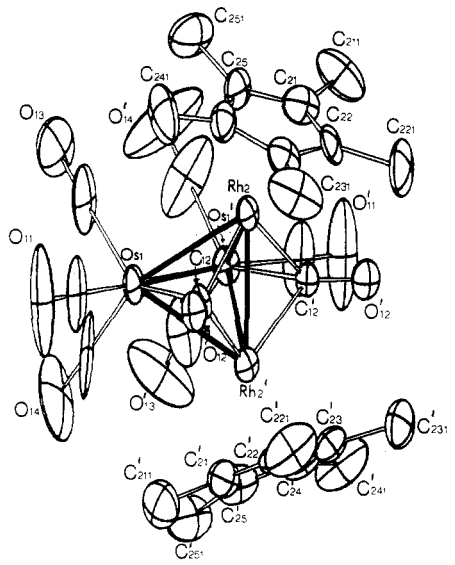

Figure 3. Molecular structure of $(\eta^5\text{-}C_5Me_5)Rh_2Os_2(CO)_8$ (50% probability ellipsoids).

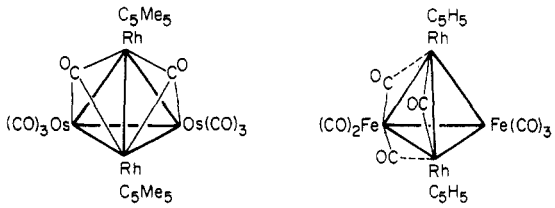

Figure 4. Arrangement of bridging carbonyls in $(\mu\text{-H})_2(\eta^5\text{-}C_5Me_5)Rh_2Os_2(CO)_8$ and in $(\mu\text{-H})_2(\eta^5\text{-Cp})Rh_2Fe_2(CO)_8$.

Scheme I

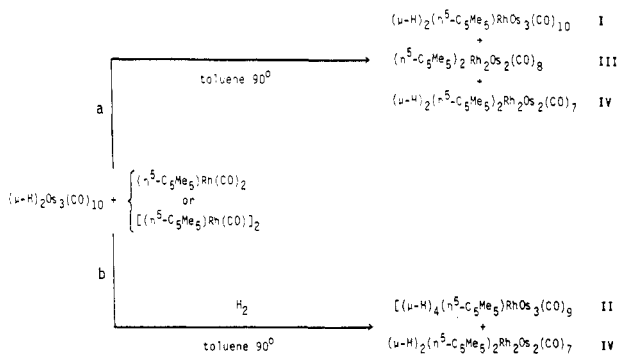

atomic scattering factors were used throughout the structure refinement with both the real and imaginary components of the anomalous dispersion included for all atoms. The heavy atoms first appeared on the E map. Then the positions of carbon and oxygen atoms were determined from a Fourier synthesis which was phased on the metal atoms. Full-matrix least-squares refinements were carried out by using anisotropic thermal parameters for non-hydrogen atoms. Final atomic positional parameters are given in Tables II–V. Molecular structures of cluster I–IV are depicted in Figures 1–4.

Results and Discussion

Reactions of $(\mu\text{-H})_2Os_3(CO)_{10}$ with $(\eta^5\text{-}C_5Me_5)Rh(CO)_2$ and with $[(\eta^5\text{-}C_5Me_5)Rh(CO)]_2$ in the Absence of and the Presence of Added H_2. Scheme I summarizes the results of reactions in the absence and in the presence of added H_2. Yields of products are listed in Table VI.

In the absence of added H_2 yields are similar when either $(\eta^5\text{-}C_5Me_5)Rh(CO)_2$ or $[(\eta^5\text{-}C_5Me_5)Rh(CO)_2$ is employed as a starting material. However, the reaction time is markedly shorter when the dimeric rhodium complex is employed (1 h vs. 4 days). Since the predominant product

Table I. Crystallographic Data of Clusters I through IV

	I	II	III	IV
chemical formula	$H_{17}RhOs_3C_{20}O_{10}$	$H_{19}RhOs_3C_{19}O_9$	$H_{30}Rh_2Os_2C_{28}O_8$	$H_{32}Rh_2Os_2C_{27}O_7$
mol wt	1090.7	1064.9	1080.9	1054.8
color of cryst	dark brown	black	black	black
space group	$P\bar{1}$	$P2_1/c$	$Ccca$	$P2_1/c$
molecules/unit cell	2	8	8	4
temp, °C	25	25	27	27
a, Å	10.473 (1)	17.151 (5)	15.966 (7)	10.923 (2)
b, Å	12.550 (1)	18.360 (3)	19.133 (5)	15.374 (2)
c, Å	9.598 (3)	17.413 (4)	20.701 (7)	17.869 (2)
α, deg	91.66 (2)			
β, deg	103.46 (2)	114.85 (2)		96.39 (2)
γ, deg	84.54 (1)			
V, Å^3 (unit cell)	1221.1	4974.9	6323.8	2982.0
cryst dimens, mm	0.30 × 0.42 × 0.45	0.20 × 0.25 × 0.25	0.30 × 0.40 × 0.50	0.20 × 0.40 × 0.40
ρ(calcd), g cm^{-3}	2.968	2.845	2.271	2.350
radiatn	Mo Kα	Mo Kα	Mo Kα	Mo Kα
abs coeff, cm^{-1}	162.9	159.9	90.8	96.2
max transmissn, %	99.89	99.85	99.72	98.45
min transmissn, %	60.13	59.70	60.68	50.31
scan mode	ω–2θ	ω–2θ	ω–2θ	ω–2θ
data collectn limits, deg	4–53	4–50	4–50	4–50
no. of unique reflctns	5040	8759	2977	7206
no. of reflectns used in structure refinement ($>3\sigma(I)$)	4163	5580	2093	5641
$R_F = [\sum\|\|F_o\| - \|F_c\|\|\sum\|F_o\|]$	0.034	0.041	0.053	0.042
$R_{wF} = \{\sum w(\|F_o\| - \|F_c\|)^2/\sum w\|F_o\|^2\}^{1/2}$	0.049	0.055	0.075	0.054
$w = [\{\sigma(\|F_o\|)\}^2 + (k\|F_o\|^2)]^{-1}$	k = 0.04	k = 0.03	k = 0.03	k = 0.03

is III, a cluster with an Rh_2Os_2 core, and since $[(\eta^5\text{-}C_5Me_5)Rh(CO)]_2$ will slowly form from $(\eta^5\text{-}C_5Me_5)Rh(CO)_2$ under the reaction conditions, we believe that when $(\eta^5\text{-}C_5Me_5)Rh(CO)_2$ is the starting material, it is slowly converted in situ to $[(\eta^5\text{-}C_5Me_5)Rh(CO)]_2$ which then reacts relatively rapidly with $(\mu\text{-}H)_2Os_3(CO)_{10}$ to produce III. The relatively low yields of $(\mu\text{-}H)_2(\eta^5\text{-}C_5Me_5)RhOs_3(CO)_{10}$ imply to us that scission of an Os–Os bond to produce a Rh_2Os_2 core is favored over scission of an Rh–Rh bond to produce a $RhOs_3$ core. Whereas the dirhodium–diosmium cluster III is the major product in Scheme Ia in the absence of added H_2, a corresponding reaction between $(\mu\text{-}H)_2Os_3(CO)_{10}$ and $(\eta^5\text{-}C_5H_5)Rh(CO)_2$ produces $(\eta^5\text{-}C_5H_5)RhOs_2(CO)_9$ and $(\mu\text{-}H)_2(\eta^5\text{-}C_5H_5)RhOs_3(CO)_{10}$ as the major products.[5] The greater tendency for the $(\eta^5\text{-}C_5Me_5)Rh$ group to form Rh–Rh bonds than the $(\eta^5\text{-}C_5H_5)Rh$ group is probably responsible for the difference in product distribution.[17-19]

In the presence of added H_2, $(\eta^5\text{-}C_5Me_5)Rh(CO)_2$ and also $[(\eta^5\text{-}C_5Me_5)Rh(CO)]_2$ react with $(\mu\text{-}H)_2Os_3(CO)_{10}$ to produce clusters II and IV as the major reaction products (Scheme Ib, Table VI). As in Scheme Ia, the reaction with $[(\eta^5\text{-}C_5Me_5)Rh(CO)]_2$ was complete in about 1 h compared to the reaction of $(\eta^5\text{-}C_5Me_5)Rh(CO)_2$ with $(\mu\text{-}H)_2Os_3(CO)_{10}$ which required about 4 days. That clusters with $RhOs_3$ and Rh_2Os_2 cores, II and IV, are the major products in comparable yields raises the possibility that II is formed from the reaction of an intermediate mononuclear rhodium hydride with $(\mu\text{-}H)_2Os_3(CO)_{10}$ while IV is formed from the reaction of the unsaturated rhodium dimer with $(\mu\text{-}H)_2Os_3(CO)_{10}$ and that these reactions occur at about the same rate.

While the major products of the reactions in the presence of added H_2 might be formed without initial formation of clusters I and III, the distribution of products indicates to us that at least in part clusters II and IV are formed through a sequence in which I is formed initially and is then converted to II. Similarly, III could be formed initially and then be converted to IV. In order to test these possibilities, interconversions were studied and are described below.

Scheme II

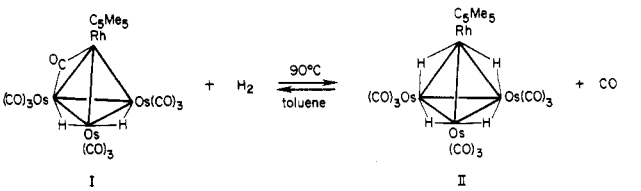

I II

Scheme III

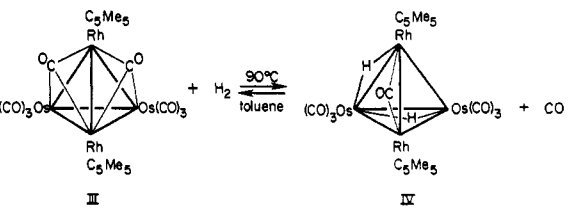

III IV

Interconversions: $(\mu\text{-}H)_2(\eta^5\text{-}C_5Me_5)RhOs_3(CO)_{10} \rightleftharpoons (\mu\text{-}H)_4(\eta^5\text{-}C_5Me_5)RhOs_3(CO)_9$ and $(\eta^5\text{-}C_5Me_5)_2Rh_2Os_2(CO)_8 \rightleftharpoons (\mu\text{-}H)_2(\eta^5\text{-}C_5Me_5)_2Rh_2Os_2(CO)_7$. Cluster I is converted to cluster II in 70% yield when H_2 at about 1 atm is placed over a solution of I at 90 °C (Scheme II). However, prolonged heating does not lead to quantitative conversion to II. The reverse reaction occurs when H_2 is replaced by CO at 1 atm above the equilibrium mixture at 90 °C, but as reductive elimination of H_2 proceeds, some decomposition of the cluster is observed after the mixture is heated for an extended period of time. Both the oxidative addition of H_2 to clusters[13] and the breakdown of the cluster skeleton[20] in the presence of CO are well-known. Analogous to the forward reaction of Scheme II, $(\mu\text{-}H)_2(\eta^5\text{-}C_5\text{-}Me_5)RhRu_3(CO)_{10}$ is converted to $(\mu\text{-}H)_4(\eta^5\text{-}C_5Me_5)RhRu_3(CO)_9$[21,22] in the presence of H_2. However,

(17) Plank, J.; Riedel, D.; Hermann, W. A. *Angew. Chem., Int. Ed. Engl.* **1980**, *19*, 937.
(18) Nulton, A.; Maitlis, P. M. *J. Organomet. Chem.* **1979**, *166*, C21.
(19) Lawson, R. J.; Shapley, J. R. *J. Am. Chem. Soc.* **1976**, *98*, 7433.
(20) Fox, J. R.; Gladfelter, W. L.; Wood, T. G.; Smegal, J. A.; Foreman, T. K.; Geoffroy, G. L.; Tavanaiepour, I.; Day, V. W.; Day, C. S. *Inorg. Chem.* **1981**, *20*, 3214.
(21) Lindsell, E. W.; Knobler, C. B.; Kaesz, H. D. *J. Organomet. Chem.* **1985**, *296*, 209.

Table II. Atomic Coordinates and Isotropic Equivalent Thermal Parameters for $(\mu\text{-}H_2)(\eta^5\text{-}C_5Me_5)RhOs_3(CO)_{10}$[a]

atom	x	y	z	B, Å²	atom	x	y	z	B, Å²
Os(1)	−0.21993 (4)	−0.12192 (4)	−0.39129 (4)	2.371 (8)	C(21)	0.068 (1)	−0.283 (1)	−0.214 (1)	4.0 (3)
Os(2)	−0.04095 (4)	−0.18096 (4)	−0.13604 (4)	2.591 (8)	C(22)	0.066 (1)	−0.192 (1)	0.057 (1)	3.5 (3)
Os(3)	−0.31081 (3)	−0.09123 (4)	−0.13110 (4)	2.410 (8)	C(23)	0.034 (1)	−0.062 (1)	−0.199 (1)	3.3 (2)
Rh(4)	−0.25913 (7)	−0.29282 (7)	−0.24113 (9)	2.48 (2)	C(31)	−0.326 (1)	−0.149 (1)	0.045 (1)	4.0 (3)
O(11)	0.8596 (9)	0.0845 (8)	0.509 (1)	4.6 (2)	C(32)	0.494 (1)	0.098 (1)	0.216 (1)	3.3 (2)
O(12)	−0.4802 (8)	−0.1123 (8)	−0.612 (1)	4.2 (2)	C(33)	−0.333 (1)	0.053 (1)	−0.070 (1)	3.1 (2)
O(13)	0.0668 (9)	0.2646 (9)	0.570 (1)	5.6 (2)	C(41)	−0.141 (1)	−0.303 (1)	−0.052 (1)	4.0 (3)
O(21)	0.1353 (9)	−0.3414 (9)	−0.263 (1)	6.3 (3)	C(110)	−0.338 (1)	−0.396 (1)	−0.442 (1)	3.7 (3)
O(22)	0.1254 (9)	−0.197 (1)	0.1706 (9)	5.2 (2)	C(111)	−0.343 (2)	−0.388 (1)	−0.600 (2)	6.4 (4)
O(23)	0.0887 (8)	0.0049 (8)	−0.2273 (9)	4.3 (2)	C(220)	−0.444 (1)	−0.355 (1)	−0.374 (1)	3.4 (2)
O(31)	−0.333 (1)	−0.183 (1)	−0.847 (1)	6.6 (3)	C(221)	−0.579 (1)	−0.305 (1)	−0.453 (2)	5.0 (3)
O(32)	0.6027 (8)	0.0973 (9)	0.263 (1)	5.1 (2)	C(330)	−0.415 (1)	−0.400 (1)	−0.233 (1)	3.3 (2)
O(33)	0.3516 (9)	0.8599 (8)	0.036 (1)	5.2 (2)	C(331)	−0.503 (1)	−0.388 (1)	−0.128 (2)	5.2 (3)
O(41)	−0.124 (1)	−0.3459 (9)	0.056 (1)	5.5 (2)	C(440)	−0.293 (1)	−0.464 (1)	−0.212 (1)	3.9 (3)
C(11)	−0.170 (1)	0.008 (1)	−0.457 (1)	3.3 (2)	C(441)	−0.235 (2)	−0.537 (1)	−0.087 (2)	5.9 (4)
C(12)	−0.382 (1)	−0.117 (1)	−0.529 (1)	3.0 (2)	C(550)	−0.244 (1)	−0.460 (1)	−0.339 (1)	3.8 (3)
C(13)	−0.124 (1)	−0.212 (1)	−0.502 (1)	3.7 (3)	C(551)	−0.122 (1)	−0.524 (1)	−0.366 (2)	5.8 (4)

[a] Esd's in parentheses.

Table III. Atomic Coordinates and Isotropic Equivalent Thermal Paremeters for $(\mu\text{-}H)_4(\eta^5\text{-}C_5Me_5)RhOs_3(CO)_9$[a]

atom	x	y	z	B, Å²	atom	x	y	z	B, Å²
				Molecule 1					
Os(1)	0.36852 (4)	0.22568 (3)	0.03330 (4)	2.82 (1)	C(411)	0.323(1)	−0.033 (1)	0.1754 (9)	4.5 (4)
Os(2)	0.27988 (4)	0.20911 (3)	0.13702 (3)	2.75 (1)	C(421)	0.125 (1)	−0.016 (1)	0.041 (1)	5.7 (5)
Os(3)	0.18053 (4)	0.21573 (3)	−0.04792 (3)	2.63 (1)	C(431)	0.121 (1)	0.003 (1)	−0.144 (1)	5.1 (5)
Rh(4)	0.27283 (7)	0.09249 (6)	0.02265 (6)	2.29 (2)	C(441)	0.316 (1)	0.005 (1)	−0.1222 (9)	4.9 (5)
C(11)	0.407 (1)	0.229 (1)	−0.054 (1)	4.9 (5)	C(451)	0.437 (1)	−0.024 (1)	0.069 (1)	4.2 (4)
C(12)	0.390 (1)	0.322 (1)	0.067 (1)	4.4 (5)	O(11)	0.4286 (9)	0.233 (1)	−0.1080 (8)	10.0 (5)
C(13)	0.479 (1)	0.192 (1)	0.116 (1)	5.4 (5)	O(12)	0.4053 (9)	0.3836 (6)	0.087 (1)	7.1 (4)
C(21)	0.206 (1)	0.186 (1)	0.191 (1)	5.3 (5)	O(13)	0.5416 (9)	0.1719 (9)	0.1631 (9)	7.4 (5)
C(22)	0.302 (1)	0.306 (1)	0.180 (1)	4.9 (5)	O(21)	0.1656 (9)	0.171 (1)	0.2246 (8)	8.3 (4)
C(23)	0.381 (1)	0.171 (1)	0.2217 (9)	4.2 (4)	O(22)	0.317 (1)	0.3639 (6)	0.2113 (8)	6.6 (4)
C(31)	0.090 (1)	0.1641 (9)	−0.0479 (9)	3.8 (4)	O(23)	0.4419 (9)	0.1476 (8)	0.2763 (9)	7.3 (5)
C(32)	0.119 (1)	0.3036 (9)	−0.096 (1)	4.5 (5)	O(31)	0.0262 (7)	0.1345 (7)	−0.0509 (8)	5.3 (3)
C(33)	0.171 (1)	0.1795 (8)	−0.1545 (9)	3.5 (4)	O(32)	0.076 (1)	0.3527 (7)	−0.1305 (8)	7.1 (5)
C(41)	0.2925 (9)	−0.0156 (8)	0.0818 (9)	2.8 (3)	O(33)	0.1678 (9)	0.1578 (8)	−0.2171 (7)	6.2 (4)
C(42)	0.2015 (9)	−0.0073 (8)	0.0230 (9)	3.5 (4)					
C(43)	0.1994 (9)	0.0003 (8)	−0.0613 (9)	3.1 (4)					
C(44)	0.2877 (9)	0.0032 (9)	−0.0549 (9)	3.3 (4)					
C(45)	0.3457 (9)	−0.0119 (9)	0.0380 (8)	3.3 (3)					
				Molecule 2					
Os(5)	0.73363 (4)	0.07930 (3)	0.40285 (4)	2.85 (1)	C(821)	0.935 (1)	0.306 (1)	0.637 (1)	6.9 (7)
Os(6)	0.69389 (4)	0.22480 (3)	0.44560 (3)	2.71 (1)	C(831)	0.857 (1)	0.213 (1)	0.753 (1)	7.8 (7)
Os(7)	0.65554 (4)	0.09263 (3)	0.51656 (4)	3.03 (1)	C(841)	0.895 (1)	0.046 (1)	0.739 (1)	6.1 (5)
Rh(8)	0.82744 (7)	0.14691 (6)	0.56428 (6)	2.49 (2)	C(851)	0.995 (1)	0.031 (1)	0.619 (1)	5.2 (5)
C(51)	0.777 (1)	−0.014 (1)	0.442 (1)	5.0 (5)	O(51)	0.809 (1)	−0.0685 (6)	0.4671 (8)	6.4 (4)
C(52)	0.792 (1)	0.0900 (8)	0.334 (1)	3.8 (4)	O(52)	0.8287 (8)	0.0959 (8)	0.2906 (8)	7.2 (4)
C(53)	0.628 (1)	0.0410 (9)	0.319 (1)	4.3 (4)	O(53)	0.5671 (9)	0.0156 (8)	0.2695 (8)	7.2 (4)
C(61)	0.782 (1)	0.2740 (9)	0.4298 (9)	4.0 (4)	O(61)	0.8369 (8)	0.3022 (8)	0.4211 (8)	6.7 (3)
C(62)	0.600 (1)	0.2719 (9)	0.3550 (9)	3.7 (4)	O(62)	0.5478 (8)	0.3041 (7)	0.3034 (7)	5.7 (4)
C(63)	0.701 (1)	0.288 (1)	0.535 (1)	4.3 (4)	O(63)	0.704 (1)	0.3249 (8)	0.5907 (8)	7.6 (4)
C(71)	0.692 (1)	−0.001 (1)	0.567 (1)	4.7 (5)	O(71)	0.719 (1)	−0.0553 (7)	0.5978 (9)	7.4 (5)
C(72)	0.620 (1)	0.124 (1)	0.599 (1)	4.2 (4)	O(72)	0.5971 (9)	0.145 (1)	0.6488 (8)	8.1 (4)
C(73)	0.546 (1)	0.053 (1)	0.440 (1)	5.1 (5)	O(73)	0.4810 (7)	0.0304 (8)	0.3986 (8)	6.0 (4)
C(81)	0.9632 (8)	0.1686 (9)	0.6051 (8)	3.1 (3)					
C(82)	0.929 (1)	0.222 (1)	0.643 (1)	4.4 (7)					
C(83)	0.895 (1)	0.183 (1)	0.6936 (9)	4.0 (4)					
C(84)	0.915 (1)	0.1077 (9)	0.6909 (9)	3.7 (4)					
C(85)	0.960 (1)	0.0991 (9)	0.638 (1)	3.7 (4)					
C(811)	1.011 (1)	0.187 (1)	0.551 (1)	5.5 (5)					

[a] Esd's in parentheses.

the reverse reaction does not occur. In the presence of CO $(\mu\text{-}H)_4(\eta^5\text{-}C_5Me_5)RhRu_3(CO)_9$ rapidly decomposes.[21,22]

Interconversion between III and IV was also observed (Scheme III). By contrast, both the oxidative addition and reductive elimination steps proceed quantitatively while decomposition of the clusters appears to be negligible. Additionally, the reverse step appears to take place faster than that of the forward step.

$(\mu\text{-}H)_2(\eta^5\text{-}C_5Me_5RhOs_3(CO)_{10}$ (I). The molecular structure of cluster I is shown in Figure 1. Selected bond distances and bond angles are given in Tables VII and VIII. It consists of a tetrahedral $RhOs_3$ metal framework in which each osmium is linked to three terminal carbonyl ligands. The rhodium is attached to a C_5Me_5 ring,.and an asymmetric bridging carbonyl spans the Os(2)–Rh(4) bond with carbon metal distances of Os(2)–C(41) = 2.206 (5) Å and Rh(4)–C(41) = 1.942 (3) Å. Although the positions

(22) Lindsell, E. W.; Knobler, C. B.; Kaesz, H. D. *J. Chem. Soc., Chem. Commun.* **1985**, 1171.

Table IV. Atomic Coordinates and Isotropic Equivalent Thermal Parameters for $(\eta^5\text{-}C_5Me_5)_2Rh_2Os_2(CO)_8$[a]

atom	x	y	z	B, Å²
Os(1)	0.83202 (4)	0.02020 (3)	0.18890 (3)	2.72 (1)
Rh(2)	0.77434 (7)	−0.06741 (5)	0.09396 (5)	2.35 (2)
O(11)	1.013 (1)	0.065 (1)	0.1696 (7)	12.0 (6)
O(12)	0.8988 (6)	0.0379 (5)	0.0486 (5)	3.1 (2)
O(13)	0.694 (1)	−0.133 (1)	0.2881 (8)	11.8 (5)
O(14)	0.889 (1)	−0.0897 (9)	0.2841 (9)	12.4 (5)
C(11)	0.944 (1)	0.048 (1)	0.1782 (8)	6.0 (5)
C(12)	0.6584 (8)	−0.0233 (7)	0.0847 (7)	2.2 (3)
C(13)	0.813 (1)	0.088 (1)	0.2520 (9)	5.8 (5)
C(14)	0.867 (1)	−0.050 (1)	0.247 (1)	6.1 (4)
C(21)	0.876 (1)	−0.1429 (9)	0.0727 (8)	4.1 (4)
C(22)	0.842 (1)	−0.1233 (8)	0.0122 (8)	3.6 (3)
C(23)	0.757 (1)	−0.1424 (8)	0.0099 (8)	3.6 (3)
C(24)	0.737 (1)	−0.1756 (8)	0.0714 (8)	4.0 (4)
C(25)	0.811 (1)	−0.1770 (9)	0.1084 (8)	4.5 (4)
C(211)	0.967 (1)	−0.135 (1)	0.091 (1)	6.9 (6)
C(221)	0.888 (1)	−0.089 (1)	−0.0437 (9)	6.4 (5)
C(231)	0.699 (1)	−0.136 (1)	−0.046 (1)	6.8 (5)
C(241)	0.655 (1)	−0.210 (1)	0.088 (1)	8.0 (6)
C(251)	0.821 (2)	−0.216 (1)	0.173 (1)	9.6 (9)

[a] Esd's in parentheses.

of the two hydrogen atoms were not determined directly from the X-ray data, they are inferred as edge bridging between Os(1)–Os(3) and Os(2)–Os(3). The distances Os(1)–Os(3) = 2.876 (1) and Os(2)–Os(3) = 2.952 (1) Å are significantly longer than the remaining osmium–osmium bond in the cluster: Os(1)–Os(2) = 2.787 (1) Å. These osmium–osmium distances correspond very well with those observed in the related cluster $(\mu\text{-}H)_2(\eta^5\text{-}C_5H_5)CoOs_3(CO)_{10}$[2] which has a molecular structure very similar to that of I. The rhodium–osmium distances are relatively uniform: Rh(4)–Os(1) = 2.734 (1), Rh(4)–Os(2) = 2.769 (1), and Rh(4)–Os(3) = 2.769 (1) Å. Reported non-hydrogen-bridged Rh–Os bonds observed in other clusters: $(\eta^5\text{-}C_5H_5)RhOs_2(CO)_9$,[5] 2.7589 (5), 2.7673 (6) Å; $(\mu\text{-}H)_2RhOs_3(acac)(CO)_{10}$ (acac = acetylacetone), 2.743 (2) Å.[23] The dihedral angle between the C_5Me_5 ring and the Os(1)–Os(2)–Os(3) plane of I is 17.8°.

Suggested positions of the bridging hydrogens are also consistent with the proton NMR spectrum at −90 °C which indicates the presence of two nonequivalent bridge hydrogens (δ −16.53 and −20.08) with no apparent spin coupling with ^{103}Rh. Thus the placement of bridging hydrogens in I is most likely the same as that observed for $(\mu\text{-}H)_2(\eta^5\text{-}C_5H_5)CoOs_3(CO)_{10}$,[2] and $(\mu\text{-}H)_2(\eta^5\text{-}C_5H_5)RhRu_3(CO)_{10}$[21,22] and that proposed for $(\mu\text{-}H)_2(\eta^5\text{-}C_5H_5)RhOs_3(CO)_{10}$ on the basis of its ^1H NMR spectrum.[5] Interestingly, for the related clusters $(\mu\text{-}H)_2(\eta^5\text{-}C_5Me_4Et)CoOs_3(CO)_{10}$[24] and $(\mu\text{-}H)_2(\eta^5\text{-}C_5Me_5)RhRu_3(CO)_{10}$[21,22] the hydrogen placement is different. While one hydrogen bridges an Os–Os edge, the second hydrogen bridges one of the Co–Os or Rh–Ru edge in these compounds.

The infrared spectrum of cluster I has the same pattern as that of the related cluster $(\mu\text{-}H)_2(\eta^5\text{-}C_5H_5)RhOs_3(CO)_{10}$.[5] Owing to the greater basicity of the C_5Me_5 ring than the C_5H_5 ring, terminal carbonyl stretching frequencies are about 10 cm^{-1} lower and the stretching frequency of the carbonyl bridging Rh and Os is about 25 cm^{-1} lower for I than for the cyclopentadienyl analogue.

$(\mu\text{-}H)_4(\eta^5\text{-}C_5Me_5)RhOs_3(CO)_9$ (II). The molecular structure of cluster II is shown in Figure 2. Selected bond distances and bond angles are listed in Tables IX and X. In the unit cell there are two independent molecules of which the gross structures are the same. The molecule has approximate C_s symmetry in the solid state. It consists of a tetrahedral $RhOs_3$ unit in which each osmium atom is linked to three carbonyl ligands, and the rhodium atom is attached to a C_5Me_5 ring. Although the positions of the four hydrogen atoms were not located directly from the diffraction analysis, the positions of the hydrogens are inferred on the basis of metal–metal distances and ^1H NMR spectra described below. This structure is in accord with the structure proposed earlier for II[6] and the related cluster $(\mu\text{-}H)_4(\eta^5\text{-}C_5H_5)CoOs_3(CO)_9$.[3] The recently reported cluster $(\mu\text{-}H)_4(\eta^5\text{-}C_5Me_5)RhRu_3(CO)_9$ also has the same structure.[21,22]

For molecule 1 hydrogen-bridged pairs of metal atoms are Rh(4)–Os(1) Rh(4)–Os(2), Os(1)–Os(3), and Os(2)–Os(3). For molecule 2 the corresponding hydrogen-bridged pairs of metal atoms are Rh(8)–Os(5), Rh(8)–Os(7), Os(5)–Os(6), and Os(6)–Os(7), respectively. The average hydrogen-bridged and non-hydrogen-bridged Rh–Os distances are 2.888 [7][25] and 2.746 [6] Å,[25] respectively, while the average hydrogen-bridged and non-hydrogen-bridged Os–Os distances are 2.932 [4][25] and 2.826 [2] Å,[25] respectively. The dihedral angle between C_5Me_5 and the plane of the three Os atoms is 7.3° and 5.3°, respectively, for molecules 1 and 2.

The metal–hydride region of the proton NMR spectrum of compound II at −60 °C consists of a doublet of intensity 2 (δ −15.17 (J_{Rh-H} = 18 Hz)) assigned to bridging hydrogens which span the Rh–Os edges of the cluster and a singlet of intensity 2 (δ −19.68) assigned to two bridging hydrogens which span the Os–Os edges of the cluster. At room temperature, the two signals in the high-field region merge to give a singlet at δ −17.48. The infrared spectra of II and its cobalt analogue $(\mu\text{-}H)_4(\eta^5\text{-}C_5H_5)CoOs_3(CO)_9$[3] have the same pattern, but all the bands in II are shifted several wavenumbers lower than the corresponding ones in the cobalt analogue.

$(\eta^5\text{-}C_5Me_5)_2Rh_2Os_2(CO)_8$ (III). The molecular structure of compound III is shown in figure 3. Bond distances and bond angles are listed in Tables XI and XII. The cluster consists of a Rh_2Os_2 tetrahedral unit in which three terminal carbonyl ligands are attached to each osmium atom, a (C_5Me_5) ring is attached to each rhodium atom, and each of the two Rh_2Os triangular faces is capped by a CO, which is an unusual arrangement. The molecule has approximate C_{2v} symmetry with the C_2 axis imposed by the *Ccca* space group passing through the midpoints of the Rh–Rh and Os–Os bonds. The Os(1)–Os(1′) bond length is 2.731 (1) Å. This appears to be the shortest Os–Os distance observed to date in a tetrahedral cluster. Typical non-hydrogen-bridged Os–Os bonds are 2.822 (1) Å in $(\mu\text{-}H)_4Os_4(CO)_{11}(NCMe)$[26] and 2.825 (2) –2.827 (2) Å in $(\mu\text{-}H)_3(\eta^5\text{-}C_5H_5)WOs_3(CO)_{11}$.[27] The Rh–Rh distance in cluster III, 2.694 (1) Å, is longer than the doubly carbonyl-bridged Rh–Rh distances in $(\eta^5\text{-}C_5Me_5)_3Rh_3(CO)_3$,[28] 2.620 (2) Å, $(\eta^5\text{-}C_5H_5)_2Rh_2(CO)_3$, 2.681 (2) Å,[29] and $(\mu\text{-}H)_2(\eta^5\text{-}C_5Me_5)_3Rh_3(CO)_2$, 2.674 (1) Å.[30] The Rh–Os distances in cluster III, 2.742 (1) and 2.750 (1) Å, are in the range of distances observed in the clusters $(\eta^5\text{-}C_5H_5)RhOs_2(CO)_9$,[5] 2.7850 (7)

(23) Farrugia, L. J.; Howard, J. A.; Mitrprachachon, P.; Stone, F. G. A.; Woodward, P. *J. Chem. Soc., Dalton Trans.* **1981**, 171.
(24) Lewis, J.; Pardy, R. B. A.; Raithby, P. R. *J. Chem. Soc. Dalton Trans.* **1982**, 1509.
(25) The error estimate shown in brackets for the average distance $\bar{d}$ was obtained from the expression $[\sum_{i=1}^{n}(d_i - \bar{d})^2/(n^2 - 1)]^{1/2}$.
(26) Churchill, M. R.; Hollander, F. J. *Inorg. Chem.* **1980**, *19*, 306.
(27) Churchill, M. R.; Hollander, F. J. *Inorg. Chem.* **1979**, *18*, 161.
(28) Paulus, E. F. *Acta Crystallogr., Sect. B: Struct. Crystallogr. Cryst. Chem.* **1969**, *B25*, 2206.
(29) Mills, O. S.; Nice, J. P. *J. Organomet. Chem.* **1967**, *10*, 337.
(30) Bray, A. C.; Green, M.; Hankey, D.; Howard, J. A. K.; Johnson, O.; Stone, F. G. A. *J. Organomet. Chem.* **1985**, *281*, C12.

Table V. Atomic Coordinates and Isotropic Equivalent Thermal Parameters for $(\mu\text{-H})_2(\eta^5\text{-C}_5\text{Me}_5)_2\text{Rh}_2\text{Os}_2(\text{CO})_7$[a]

atom	x	y	z	B, Å²	atom	x	y	z	B, Å²
Os(3)	0.22758 (3)	0.19197 (2)	0.73527 (2)	2.913 (6)	C(23)	0.5527 (8)	0.1904 (7)	0.5755 (6)	4.1 (2)
Os(4)	0.16196 (3)	0.10094 (2)	0.59828 (2)	3.032 (7)	C(24)	0.5642 (8)	0.1486 (6)	0.6472 (6)	3.4 (2)
Rh(1)	0.15127 (6)	0.28064 (4)	0.61005 (3)	2.45 (1)	C(25)	0.5633 (8)	0.2138 (7)	0.7010 (5)	3.9 (2)
Rh(2)	0.37943 (6)	0.20918 (4)	0.62685 (3)	2.46 (1)	C(31)	0.290 (1)	0.2966 (6)	0.7814 (5)	4.0 (2)
O(1)	0.2791 (6)	0.2622 (5)	0.4756 (3)	3.8 (1)	C(32)	0.317 (1)	0.1211 (7)	0.8104 (5)	4.1 (2)
O(31)	0.3272 (7)	0.3579 (5)	0.8095 (4)	5.6 (2)	C(33)	0.077 (1)	0.1907 (9)	0.7783 (6)	4.9 (3)
O(32)	0.3737 (8)	0.0799 (5)	0.8533 (4)	6.0 (2)	C(41)	0.188 (1)	−0.0210 (7)	0.6054 (6)	4.8 (2)
O(33)	0.9854 (8)	0.1899 (6)	0.8076 (5)	6.9 (2)	C(42)	0.989 (1)	0.1016 (8)	0.6030 (6)	4.9 (2)
O(41)	0.1958 (9)	−0.0941 (5)	0.6086 (6)	7.8 (3)	C(43)	0.141 (1)	0.1029 (8)	0.4911 (6)	5.9 (3)
O(42)	0.8863 (7)	0.0967 (6)	0.6027 (6)	7.3 (2)	C(111)	0.848 (1)	0.2957 (9)	0.6502 (7)	5.7 (3)
O(43)	0.122 (1)	0.1032 (7)	0.4262 (5)	8.7 (3)	C(121)	0.040 (1)	0.4197 (9)	0.7455 (6)	6.4 (3)
C(1)	0.2671 (8)	0.2535 (6)	0.5379 (4)	3.1 (2)	C(131)	0.229 (1)	0.4948 (8)	0.6353 (9)	6.2 (3)
C(11)	0.9644 (8)	0.3338 (7)	0.6228 (5)	3.5 (2)	C(141)	0.135 (1)	0.4266 (7)	0.4684 (5)	5.0 (2)
C(12)	0.0511 (9)	0.3898 (6)	0.6658 (5)	3.6 (2)	C(151)	0.905 (1)	0.2957 (8)	0.4814 (6)	5.2 (3)
C(13)	0.1256 (9)	0.4270 (6)	0.6156 (6)	3.9 (2)	C(211)	0.546 (1)	0.3833 (8)	0.7049 (8)	6.9 (3)
C(14)	0.0860 (9)	0.3966 (6)	0.5396 (5)	3.4 (2)	C(221)	0.531 (1)	0.3539 (9)	0.5278 (8)	7.1 (3)
C(15)	0.9836 (9)	0.3394 (7)	0.5454 (5)	3.5 (2)	C(231)	0.562 (1)	0.151 (1)	0.4971 (7)	7.2 (3)
C(21)	0.5394 (8)	0.2945 (7)	0.6664 (6)	3.8 (2)	C(241)	0.588 (1)	0.0517 (7)	0.6598 (8)	5.7 (3)
C(22)	0.5382 (8)	0.2806 (7)	0.5871 (5)	4.0 (2)	C(251)	0.599 (1)	0.199 (1)	0.7860 (7)	7.0 (4)

[a] Esd's in parentheses.

Table VI. Product Distribution in the Reaction of $H_2Os_3(CO)_{10}$ with $(\eta^5\text{-C}_5\text{Me}_5)\text{Rh}(CO)_2$ or $[(\eta^5\text{-C}_5\text{Me}_5)\text{Rh}(CO)]_2$ in the Absence and Presence (in Parentheses) of H_2

	$(\eta^5\text{-C}_5\text{Me}_5)$-Rh(CO)₂	$[(\eta^5\text{-C}_5\text{Me}_5)$-Rh(CO)]₂
$H_2(\eta^5\text{-C}_5\text{Me}_5)\text{RhOs}_3(CO)_{10}$ (I)	12 (...)	7 (4)
$H_4(\eta^5\text{-C}_5\text{Me}_5)\text{RhOs}_2(CO)_9$ (II)	... (36)	... (18)
$(\eta^5\text{-C}_5\text{Me}_5)_2\text{Rh}_2\text{Os}_2(CO)_8$ (III)	40 (...)	42 (...)
$H_2(\eta^5\text{-C}_5\text{Me}_5)_2\text{Rh}_2\text{Os}_2(CO)_7$ (IV)	7 (36)	7 (25)

Table VII. Selected Bond Distances (Å)[a,b] of $(\mu\text{-H})_2(\eta^5\text{-C}_5\text{Me}_5)\text{RhOs}_3(CO)_{10}$

M–M Distances			
Os(1)–Os(2)	2.787 (1)	Os(1)–Rh(4)	2.734 (1)
Os(1)–Os(3)	2.876 (1)	Os(2)–Rh(4)	2.769 (1)
Os(2)–Os(3)	2.952 (1)	Os(3)–Rh(4)	2.769 (1)
Os–CO and Rh–CO Distances			
Os(1)–C(11)	1.923 (4)	Os(3)–C(31)	1.899 (4)
Os(1)–C(12)	1.890 (9)	Os(3)–C(32)	1.909 (7)
Os(1)–C(13)	1.900 (4)	Os(3)–C(33)	1.901 (1)
Os(2)–C(21)	1.890 (8)	Os(2)–C(41)	2.206 (5)
Os(2)–C(22)	1.930 (2)	Rh(4)–C(41)	1.942 (3)
Os(2)–C(23)	1.932 (4)		
C–O Distances			
C(11)–O(11)	1.120 (4)	C(23)–O(23)	1.129 (6)
C(12)–O(12)	1.143 (9)	C(31)–O(31)	1.160 (4)
C(13)–O(13)	1.147 (4)	C(32)–O(32)	1.125 (12)
C(21)–O(21)	1.133 (9)	C(33)–O(33)	1.141 (2)
C(22)–O(22)	1.123 (2)	C(41)–O(41)	1.153 (1)
Rh–C_5Me_5 Distances			
Rh(4)–C(110)	2.324 (3)	Rh(4)–C(440)	2.250 (3)
Rh(4)–C(220)	2.251 (8)	Rh(4)–C(550)	2.277 (1)
Rh(4)–C(330)	2.226 (5)		

[a] Intra-ring bond distances are provided in the supplementary material. [b] Esd's in parentheses.

Table VIII. Selected Bond Angles (deg)[a,b] of $(\mu\text{-H})_2(\eta^5\text{-C}_5\text{Me}_5)\text{RhOs}_3(CO)_{10}$

Angles within $RhOs_3$ Cluster			
Os(2)–Os(1)–Os(3)	62.81 (1)	Os(1)–Os(3)–Os(2)	57.13 (1)
Os(2)–Os(1)–Rh(4)	60.20 (1)	Os(1)–Os(3)–Rh(4)	57.91 (1)
Os(3)–Os(1)–Rh(4)	59.09 (1)	Os(1)–Os(3)–Rh(4)	57.80 (1)
Os(1)–Os(2)–Os(3)	60.06 (1)	Os(1)–Rh(4)–Os(2)	60.85 (1)
Os(1)–Os(2)–Rh(4)	58.95 (1)	Os(1)–Rh(4)–Os(3)	63.00 (1)
Os(3)–Os(2)–Rh(4)	57.79 (1)	Os(2)–Rh(4)–Os(3)	64.41 (1)
Metal–Metal–Carbon (CO) Angles			
Os(2)–Os(1)–C(11)	108.16 (15)	Rh(4)–Os(2)–C(23)	135.93 (12)
Os(2)–Os(1)–C(12)	156.24 (20)	Os(1)–Os(3)–C(31)	148.10 (17)
Os(2)–Os(1)–C(13)	92.25 (9)	Os(1)–Os(3)–C(32)	96.58 (9)
Os(3)–Os(1)–C(11)	112.55 (9)	Os(1)–Os(3)–C(33)	115.19 (19)
Os(3)–Os(1)–C(12)	100.78 (24)	Os(2)–Os(3)–C(31)	99.62 (33)
Os(3)–Os(1)–C(13)	147.71 (1)	Os(2)–Os(3)–C(32)	144.79 (7)
Rh(4)–Os(1)–C(11)	157.42 (8)	Os(2)–Os(3)–C(33)	117.36 (36)
Rh(4)–Os(1)–C(12)	97.08 (16)	Rh(4)–Os(3)–C(31)	91.95 (7)
Rh(4)–Os(1)–C(13)	91.44 (7)	Rh(4)–Os(3)–C(32)	89.19 (5)
Os(1)–Os(2)–C(21)	97.55 (14)	Rh(4)–Os(3)–C(33)	172.73 (28)
Os(1)–Os(2)–C(22)	166.89 (9)	Os(1)–Os(2)–C(41)	102.32 (12)
Os(1)–Os(2)–C(23)	77.01 (13)	Os(3)–Os(2)–C(41)	71.13 (16)
Os(3)–Os(2)–C(21)	147.87 (19)	Rh(4)–Os(2)–C(41)	44.16 (10)
Os(3)–Os(2)–C(22)	109.84 (17)	Os(1)–Rh(4)–C(41)	112.18 (13)
Os(3)–Os(2)–C(23)	102.95 (18)	Os(2)–Rh(4)–C(41)	52.31 (16)
Rh(4)–Os(2)–C(21)	91.52 (31)	Os(3)–Rh(4)–C(41)	78.89 (7)
Rh(4)–Os(2)–C(22)	124.67 (14)		
Metal–C–O Angles			
Os(1)–C(11)–O(11)	177.98 (5)	Os(3)–C(31)–O(31)	178.66 (57)
Os(1)–C(12)–O(12)	179.05 (1)	Os(3)–C(32)–O(32)	176.41 (16)
Os(1)–C(13)–O(13)	178.85 (6)	Os(3)–C(33)–O(33)	177.18 (95)
Os(2)–C(21)–O(21)	178.24 (56)	Os(2)–C(41)–O(41)	134.33 (60)
Os(2)–C(22)–O(22)	178.02 (47)	Rh(4)–C(41)–O(41)	142.15 (65)
Os(2)–C(23)–O(23)	173.68 (6)		
Carbon (CO)–Metal–Carbon (CO) Angles			
C(11)–Os(1)–C(12)	93.75 (22)	C(31)–Os(3)–C(32)	92.82 (35)
C(11)–Os(1)–C(13)	93.90 (18)	C(31)–Os(3)–C(33)	94.34 (13)
C(12)–Os(1)–C(13)	95.37 (23)	C(32)–Os(3)–C(33)	94.13 (32)
C(21)–Os(2)–C(22)	94.98 (21)	C(21)–Os(2)–C(41)	94.14 (27)
C(21)–Os(2)–C(23)	92.76 (28)	C(22)–Os(2)–C(41)	80.54 (17)
C(22)–Os(2)–C(23)	98.59 (15)	C(23)–Os(2)–C(41)	173.10 (18)

[a] Intra-ring bond angles are provided in the supplementary material. [b] Esd's in parentheses.

and 2.7673 (6) Å, $(\mu\text{-H})_2\text{RhOs}_3(\text{acac})(CO)_{10}$,[23] 2.743 (2) Å, and $(\mu\text{-H})_2(\eta^5\text{-C}_5\text{Me}_5)\text{RhOs}_3(CO)_{10}$, 2.731 (1) – 2.769 (1) Å. The dihedral angle between the C_5Me_5 planes in cluster III is 45.9°.

Bands at 1674 and 1698 cm^{-1} in the IR spectrum and a triplet at δ 240.18 (J_{Rh-C} = 34 Hz) in the ^{13}C NMR spectrum of III are assigned to the face-bridging carbonyls.

The cluster $(\eta^5\text{-C}_5\text{H}_5)_2\text{Rh}_2\text{Fe}_2(CO)_8$[31] is an isoelectronic analogue of III. However, unlike III, it has no face-bridging carbonyls. Instead, there are three edge-bridging carbonyls, one across a Rh–Rh edge and carbonyl bridges across two Rh–Fe edges. Figure 4 compares the arrangement of bridging carbonyls in III with the bridging carbonyl arrangement in $(\eta^5\text{-C}_5\text{H}_5)_2\text{Rh}_2\text{Fe}_2(CO))_8$.[32]

(31) Knight, J.; Mays, M. J. *J. Chem. Soc. A* **1970**, 654.

(32) Churchill, R.; Veidis, M. V. *J. Chem. Soc. A* **1970**, 2170.

Table IX. Selected Bond Distances (Å)[a,b] of $(\mu\text{-H})_4(\eta^5\text{-}C_5Me_5)RhOs_3(CO)_9$

molecule 1		molecule 2	
Metal–Metal Distances			
Os(1)–Os(2)	2.823 (1)	Os(5)–Os(6)	2.930 (1)
Os(1)–Os(3)	2.931 (1)	Os(5)–Os(7)	2.829 (1)
Os(1)–Rh(4)	2.907 (1)	Os(5)–Rh(8)	2.868 (1)
Os(2)–Os(3)	2.944 (1)	Os(6)–Os(7)	2.921 (1)
Os(2)–Rh(4)	2.892 (1)	Os(6)–Rh(8)	2.753 (1)
Os(3)–Rh(4)	2.739 (1)	Os(7)–Rh(8)	2.884 (1)
Rh–C of C_5Me_5 Distances			
Rh(4)–C(41)	2.19 (1)	Rh(8)–C(81)	2.17 (1)
Rh(4)–C(42)	2.20 (1)	Rh(8)–C(82)	2.19 (1)
Rh(4)–C(43)	2.24 (1)	Rh(8)–C(83)	2.16 (1)
Rh(4)–C(44)	2.21 (1)	Rh(8)–C(84)	2.20 (1)
Rh(4)–C(45)	2.24 (1)	Rh(8)–C(85)	2.26 (2)
Os–C of CO Distances			
Os(1)–C(11)	1.89 (2)	Os(5)–C(51)	1.88 (2)
Os(1)–C(12)	1.86 (2)	Os(5)–C(52)	1.87 (2)
Os(1)–C(13)	1.94 (2)	Os(5)–C(53)	1.92 (2)
Os(2)–C(21)	1.92 (2)	Os(6)–C(61)	1.87 (2)
Os(2)–C(22)	1.91 (2)	Os(6)–C(62)	1.92 (2)
Os(2)–C(23)	1.87 (2)	Os(6)–C(63)	1.91 (2)
Os(3)–C(31)	1.81 (2)	Os(7)–C(71)	1.92 (2)
Os(3)–C(32)	1.92 (2)	Os(7)–C(72)	1.88 (2)
Os(3)–C(33)	1.910 (15)	Os(7)–C(73)	1.94 (2)
C–O Distances			
C(11)–O(11)	1.15 (2)	C(51)–O(51)	1.13 (2)
C(12)–O(12)	1.17 (2)	C(52)–O(52)	1.17 (2)
C(13)–O(13)	1.10 (2)	C(53)–O(53)	1.14 (2)
C(21)–O(21)	1.11 (2)	C(61)–O(61)	1.14 (2)
C(22)–O(22)	1.17 (2)	C(62)–O(62)	1.13 (2)
C(23)–O(23)	1.16 (2)	C(63)–O(63)	1.16 (2)
C(31)–O(31)	1.21 (2)	C(71)–O(71)	1.13 (2)
C(32)–O(32)	1.16 (2)	C(72)–O(72)	1.15 (2)
C(33)–O(33)	1.14 (2)	C(73)–O(73)	1.12 (2)

[a] Intra-ring bond distances are provided in the supplementary material. [b] Esd's in parentheses.

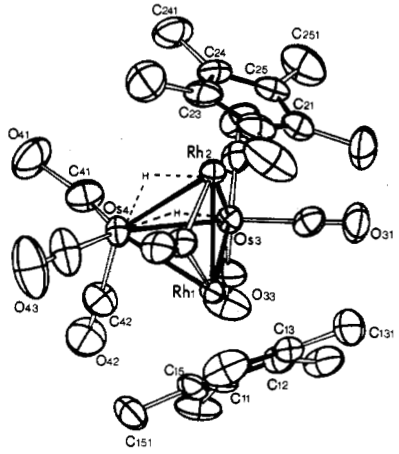

Figure 5. Molecular structure of $(\mu\text{-H})_2(\eta^5\text{-}C_5Me_5)Rh_2Os_2(CO)_7$ (50% probability ellipsoids).

$(\mu\text{-H})_2(\eta^5\text{-}C_5Me_5)_2Rh_2Os_2(CO)_7$ (IV). The molecular structure of IV is shown in Figure 5. Selected bond distances and bond angles are listed in Tables XIII and XIV. The molecule consists of a tetrahedral Rh_2Os_2 unit in which three carbonyl ligands are attached to each osmium atom, a (C_5Me_5) ring is attached to each rhodium atom, and a bridging carbonyl spans the two rhodium atoms. Although the positions of the hydrogen atoms were not directly determined, they are inferred as hydrogen bridges in Os(3)–H–Os(4) and Rh(2)–H–Os(4) angles by comparison of metal–metal distances and bond angles around the Os(4) atom. Thus the distances Os(3)–Os(4) = 2.844 (1) Å and Rh(2)–Os(4) = 2.901 (1) Å are significantly longer than the other metal–metal distances in the molecule. Consistent with the suggested Os(4)–H–Rh(2) bond is the significantly larger angle Rh(2)–Os(4)–C(41) = 116.1 (3)° than Rh(1)–Os(4)–C(42) = 86.6 (3)°. This difference is

Table X. Selected Bond Angles (Å)[a,b] of $(\mu\text{-H})_4(\eta^5\text{-}C_5Me_5)RhOs_3(CO)_9$

molecule 1		molecule 2	
Angles within $RhOs_3$ Cluster			
Os(2)–Os(1)–Os(3)	61.51 (2)	Os(6)–Os(5)–Os(7)	60.93 (3)
Os(2)–Os(1)–Rh(4)	60.60 (2)	Os(6)–Os(5)–Rh(8)	56.69 (3)
Os(3)–Os(1)–Rh(4)	55.96 (2)	Os(7)–Os(4)–Rh(8)	60.82 (3)
Os(1)–Os(2)–Os(3)	61.05 (2)	Os(5)–Os(6)–Os(7)	57.82 (3)
Os(1)–Os(2)–Rh(4)	61.13 (2)	Os(5)–Os(6)–Rh(8)	60.51 (3)
Os(3)–Os(2)–Rh(4)	55.98 (2)	Os(7)–Os(6)–Rh(8)	61.00 (3)
Os(1)–Os(3)–Os(2)	57.44 (2)	Os(5)–Os(7)–Os(6)	61.25 (3)
Os(1)–Os(3)–Rh(4)	61.57 (2)	Os(5)–Os(7)–Rh(8)	60.26 (3)
Os(2)–Os(3)–Rh(4)	61.05 (2)	Os(6)–Os(7)–Rh(8)	56.62 (3)
Os(1)–Rh(4)–Os(2)	58.27 (2)	Os(5)–Rh(8)–Os(6)	62.80 (3)
Os(1)–Rh(4)–Os(3)	62.47 (3)	Os(5)–Rh(8)–Os(7)	58.92 (2)
Os(2)–Rh(4)–Os(3)	62.97 (2)	Os(6)–Rh(8)–Os(7)	62.38 (3)
Os–Os–C Angles			
Os(2)–Os(1)C(11)	168.3 (5)	Os(6)–Os(5)–C(51)	147.2 (5)
Os(2)–Os(1)–C(12)	89.3 (5)	Os(6)–Os(5)–C(52)	108.2 (4)
Os(2)–Os(1)–C(13)	96.4 (6)	Os(6)–Os(5)–C(53)	106.3 (5)
Os(3)–Os(1)–C(11)	107.5 (5)	Os(7)–Os(5)–C(51)	93.3 (6)
Os(3)–Os(1)–C(12)	104.1 (5)	Os(7)–Os(5)–C(52)	168.3 (4)
Os(3)–Os(1)–C(13)	150.8 (6)	Os(7)–Os(5)–C(53)	89.5 (5)
Rh(4)–Os(1)–C(11)	110.6 (5)	Rh(8)–Os(5)–C(51)	94.1 (5)
Rh(4)–Os(1)–C(12)	148.8 (5)	Rh(8)–Os(5)–C(52)	110.4 (5)
Rh(4)–Os(1)–C(13)	97.5 (6)	Rh(8)–Os(5)–C(53)	149.9 (5)
Os(1)–Os(2)–C(21)	169.0 (5)	Os(5)–Os(6)–C(61)	96.6 (4)
Os(1)–Os(2)–C(22)	94.4 (5)	Os(5)–Os(6)–C(62)	114.0 (4)
Os(1)–Os(2)–C(23)	88.6 (4)	Os(5)–Os(6)–C(63)	145.3 (5)
Os(3)–Os(2)–C(21)	110.1 (5)	Os(7)–Os(6)–C(61)	143.2 (5)
Os(3)–Os(2)–C(22)	108.7 (5)	Os(7)–Os(6)–C(62)	117.4 (4)
Os(3)–Os(2)–C(23)	142.7 (4)	Os(7)–Os(6)–C(63)	96.2 (5)
Rh(4)–Os(2)–C(21)	108.9 (6)	Rh(8)–Os(6)–C(61)	83.9 (5)
Rh(4)–Os(2)–C(22)	154.9 (5)	Rh(8)–Os(6)–C(62)	174.4 (4)
Rh(4)–Os(2)–C(23)	91.5 (5)	Rh(8)–Os(6)–C(63)	87.6 (5)
Os(1)–Os(3)–C(31)	142.9 (5)	Os(5)–Os(7)–C(71)	94.8 (5)
Os(1)–Os(3)–C(32)	116.7 (5)	Os(5)–Os(7)–C(72)	165.2 (5)
Os(1)–Os(3)–C(33)	96.9 (5)	Os(5)–Os(7)–C(73)	95.2 (5)
Os(2)–Os(3)–C(31)	94.6 (4)	Os(6)–Os(7)–C(71)	148.5 (5)
Os(2)–Os(3)–C(32)	118.3 (5)	Os(6)–Os(7)–C(72)	105.8 (5)
Os(2)–Os(3)–C(33)	145.2 (4)	Os(6)–Os(7)–C(73)	110.3 (4)
Rh(4)–Os(3)–C(31)	84.3 (5)	Rh(8)–Os(7)–C(71)	94.6 (5)
Rh(4)–Os(3)–C(32)	178.2 (5)	Rh(8)–Os(7)–C(72)	107.3 (5)
Rh(4)–Os(3)–C(33)	86.9 (4)	Rh(8)–Os(7)–C(73)	155.2 (5)
Carbon–Osmium–Carbon Angles			
C(11)–Os(1)–C(12)	97.8 (7)	C(51)–Os(5)–C(52)	95.1 (2)
C(11)–Os(1)–C(13)	92.4 (7)	C(51)–Os(5)–C(53)	92.3 (7)
C(12)–Os(1)–C(13)	93.8 (7)	C(52)–Os(5)–C(53)	98.3 (7)
C(21)–Os(2)–C(22)	94.8 (8)	C(61)–Os(6)–C(62)	96.5 (6)
C(21)–Os(2)–C(23)	96.6 (7)	C(61)–Os(6)–C(63)	92.9 (6)
C(22)–Os(2)–C(23)	93.9 (7)	C(62)–Os(6)–C(63)	97.9 (6)
C(31)–Os(3)–C(32)	97.4 (7)	C(71)–Os(7)–C(72)	94.2 (7)
C(31)–Os(3)–C(33)	95.2 (6)	C(71)–Os(7)–C(73)	90.8 (7)
C(32)–Os(3)–C(33)	93.3 (6)	C(72)–Os(7)–C(73)	96.4 (7)
Os–C–O Angles			
Os(1)–C(11)–O(11)	177 (2)	Os(5)–C(51)–O(51)	175 (2)
Os(1)–C(12)–O(12)	177 (2)	Os(5)–C(52)–O(52)	179 (2)
Os(1)–C(13)–O(13)	179 (2)	Os(5)–C(53)–O(53)	177 (2)
Os(2)–C(21)–O(21)	177 (2)	Os(6)–C(61)–O(61)	178 (1)
Os(2)–C(22)–O(22)	176 (1)	Os(6)–C(62)–O(62)	175 (1)
Os(2)–C(23)–O(23)	178 (1)	Os(6)–C(63)–O(63)	178 (2)
Os(3)–C(31)–O(31)	175 (1)	Os(7)–C(71)–O(71)	175 (2)
Os(3)–C(32)–O(32)	174 (2)	Os(7)–C(72)–O(72)	178 (2)
Os(3)–C(33)–O(33)	178 (1)	Os(7)–C(73)–O(73)	176 (2)

[a] Intra-ring bond angles are provided in the supplementary material. [b] Esd's in parentheses.

Table XI. Selected Bond Distances (Å)[a,b] of $(\eta^5\text{-}C_5Me_5)_2Rh_2Os_2(CO)_8$

	Metal–Metal Distances		
Os(1)–Os(1′)	2.731 (1)	Os(1)–Rh(2′)	2.750 (1)
Os(1)–Rh(2)	2.742 (1)	Rh(2)–Rh(2′)	2.694 (1)
	Rh–C of C_5Me_5 Distances		
Rh(2)–C(21)	2.218 (10)	Rh(2)–C(24)	2.205 (8)
Rh(2)–C(22)	2.274 (8)	Rh(2)–C(25)	2.199 (10)
Rh(2)–C(23)	2.273 (8)		
	Metal–C of CO Distances		
Os(1)–C(11)	1.871 (12)	Os(1)–C(12)	2.164 (8)
Os(1)–C(13)	1.860 (11)	Rh(2)–C(12)	2.043 (7)
Os(1)–C(14)	1.880 (11)		
	C–O Distances		
C(11)–O(11)	1.165 (13)	C(13)–O(13)	1.152 (14)
C(12)–O(12)	1.212 (9)	C(14)–O(14)	1.144 (13)

[a] Intra-ring bond distances are provided in the supplementary material. [b] Esd's in parentheses.

Table XII. Selected Bond Angles (Å)[a,b] of $(\eta^5\text{-}C_5Me_5)_2Rh_2Os_2(CO)_8$

	Angles within Rh_2Os_2 Cluster		
Os(1′)–Os(1)–Rh(2)	60.32 (2)	Os(1)–Rh(2)–Os(1′)	59.63 (2)
Os(1′)–Os(1)–Rh(2′)	60.05 (2)	Os(1)–Rh(2)–Rh(2′)	60.77 (2)
Rh(2)–Os(1)–Rh(2′)	58.75 (2)	Os(1′)–Rh(2)–Rh(2′)	60.49 (2)
	Metal–Metal–Carbon Angles		
Os(1′)–Os(1)–C(11)	173.2 (3)	Rh(2)–Os(1)–C(11)	114.0 (4)
Os(1′)–Os(1)–C(12)	94.3 (2)	Rh(2)–Os(1)–C(12)	47.6 (2)
Os(1′)–Os(1)–C(13)	92.2 (4)	Rh(2)–Os(1)–C(13)	150.7 (4)
Os(1′)–Os(1)–C(14)	94.5 (4)	Rh(2)–Os(1)–C(14)	96.8 (3)
Rh(2′)–Os(1)–C(11)	114.3 (3)	Os(1)–Rh(2)–C(12)	51.1 (2)
Rh(2′)–Os(1)–C(12)	47.3 (2)	Os(1)–Rh(2)–C(12′)	96.9 (2)
Rh(2′)–Os(1)–C(13)	100.0 (3)	Os(1′)–Rh(2)–C(12)	96.5 (2)
Rh(2′)–Os(1)–C(14)	150.5 (3)	Os(1′)–Rh(2)–C(12′)	51.2 (2)
		Rh(2′)–Rh(2)–C(12)	49.0 (2)
		Rh(2′)–Rh(2)–C(12′)	48.7 (2)
	Carbon–Metal–Carbon Angles		
C(11)–Os(1)–C(12)	78.9 (3)	C(12)–Rh(2)–C(12′)	96.7 (3)
C(11)–Os(1)–C(13)	92.6 (6)		
C(11)–Os(1)–C(14)	89.7 (5)		
C(12)–Os(1)–C(13)	133.8 (4)		
C(12)–Os(1)–C(14)	129.3 (5)		
C(13)–Os(1)–C(14)	95.5 (6)		
	Metal–Carbon–Oxygen Angles		
Os(1)–C(11)–O(11)	177.8 (9)	Os(1)–C(12)–O(12)	132.3 (6)
Os(1)–C(13)–O(13)	174 (1)	Rh(2)–C(12)–O(12)	130.2 (6)
Os(1)–C(14)–O(14)	176 (1)	Rh(2′)–C(12)–O(12)	130.0 (6)

[a] Intra-ring bond angles are provided in the supplementary material. [b] Esd's in parentheses.

apparent in Figure 5. Furthermore, an appreciable difference in dihedral angles involving the C_5Me_5 planes is observed. The dihedral angle between the C(11)–C(12)–C(13)–C(14)–C(15) plane and the Rh(2)–Os(3)–Os(4) plane is 44.4°, while the dihedral angle between the C(21)–C(22)–C(23)–C(24)–C(25) plane and the Rh(1)–Os(3)–Os(4) plane is 15.8°. The dihedral angle between the C(11)–C(12)–C(13)–C(14)–C(15) and C(21)–C(22)–C(23)–C(24)–C(25) planes is 76.4°.

The arrangement of the hydrogen atoms is further confirmed by the proton NMR spectrum of compound IV in CD_2Cl_2 at −90 °C. A singlet of intensity 1 at δ −14.57 is assigned to the bridging hydrogen along the Os–Os bond, while a doublet of intensity 1 at δ −18.80 (J_{Rh-H} = 26 Hz) is assigned to the bridging hydrogen across the Rh–Os bond. The distance Os(3)–Os(4) = 2.844 (1) Å is about 0.1 Å shorter than usually observed for hydrogen-bridged Os–Os bonds: 2.941 (2) Å in $(\mu\text{-}H)_3(\eta^5\text{-}C_5H_5)WOs_3(CO)_{11}$,[27] 2.932 (2) Å in $(\mu\text{-}H)(\eta^5\text{-}C_5H_5)WOs_3(CO)_{12}$,[33] and 2.956 (1) −2.971 (1) Å in $(\mu\text{-}H)_4Os_4(CO)_{11}(NCMe)$.[26]

Table XIII. Selected Bond Distances (Å)[a,b] of $(\mu\text{-}H)_2(\eta^5\text{-}C_5Me_5)_2Rh_2Os_2(CO)_7$

	Metal–Metal Distances		
Rh(1)–Rh(2)	2.712 (1)	Rh(2)–Os(3)	2.700 (1)
Rh(1)–Os(3)	2.675 (1)	Rh(2)–Os(4)	2.901 (1)
Rh(1)–Os(4)	2.775 (1)	Os(3)–Os(4)	2.844 (1)
	Rh–C of C_5Me_5 Distances		
Rh(1)–C(11)	2.235 (6)	Rh(2)–C(21)	2.237 (7)
Rh(1)–C(12)	2.291 (6)	Rh(2)–C(22)	2.235 (6)
Rh(1)–C(13)	2.272 (7)	Rh(2)–C(23)	2.212 (6)
Rh(1)–C(14)	2.254 (6)	Rh(2)–C(24)	2.217 (7)
Rh(1)–C(15)	2.246 (6)	Rh(2)–C(25)	2.284 (6)
	Metal–C of CO Distances		
Rh(1)–C(1)	1.949 (6)	Rh(2)–C(1)	2.018 (6)
Os(3)–C(31)	1.902 (8)	Os(4)–C(41)	1.900 (7)
Os(3)–C(32)	1.915 (7)	Os(4)–C(42)	1.905 (8)
Os(3)–C(33)	1.890 (9)	Os(4)–C(43)	1.905 (8)
	C–O Distances		
C(31)–O(31)	1.122 (8)	C(41)–O(41)	1.128 (9)
C(32)–O(32)	1.124 (10)	C(42)–O(42)	1.120 (11)
C(33)–O(33)	1.182 (12)	C(43)–O(43)	1.156 (9)
C(1)–O(1)	1.145 (7)		

[a] Intra-ring bond distances are provided in the supplementary material. [b] Esd's in parentheses.

Table XIV. Selected Bond Angles (deg)[a,b] of $(\mu\text{-}H)_2(\eta^5\text{-}C_5Me_5)_2Rh_2Os_2(CO)_7$

	Angles within Rh_2Os_2 Cluster		
Rh(2)–Rh(1)–Os(3)	60.16 (1)	Rh(1)–Os(3)–Rh(2)	60.58 (1)
Rh(2)–Rh(1)–Os(4)	63.83 (1)	Rh(1)–Os(3)–Os(4)	60.27 (1)
Os(3)–Rh(1)–Os(4)	62.88 (1)	Rh(2)–Os(3)–Os(4)	63.03 (1)
Rh(1)–Rh(2)–Os(3)	59.26 (1)	Rh(1)–Os(4)–Rh(2)	57.03 (1)
Rh(1)–Rh(2)–Os(4)	59.15 (1)	Rh(1)–Os(4)–Os(3)	56.85 (1)
Os(3)–Rh(2)–Os(4)	60.91 (1)	Rh(2)–Os(4)–Os(3)	56.06 (1)
	Metal–Metal–Carbon Angles		
Rh(2)–Rh(1)–C(1)	47.9 (2)	Rh(1)–Rh(2)–C(1)	45.8 (2)
Os(3)–Rh(1)–C(1)	106.2 (2)	Os(3)–Rh(2)–C(1)	103.3 (2)
Os(4)–Rh(1)–C(1)	72.6 (2)	Os(4)–Rh(2)–C(1)	68.9 (2)
Rh(1)–Os(3)–C(31)	89.8 (2)	Rh(1)–Os(4)–C(41)	170.2 (3)
Rh(1)–Os(3)–C(32)	165.0 (2)	Rh(1)–Os(4)–C(42)	86.6 (3)
Rh(1)–Os(3)–C(33)	98.1 (3)	Rh(1)–Os(4)–C(43)	93.4 (3)
Rh(2)–Os(3)–C(31)	90.4 (2)	Rh(2)–Os(4)–C(41)	116.1 (3)
Rh(2)–Os(3)–C(32)	104.5 (2)	Rh(2)–Os(4)–C(42)	142.0 (3)
Rh(2)–Os(3)–C(33)	157.5 (3)	Rh(2)–Os(4)–C(43)	100.0 (3)
Os(4)–Os(3)–C(31)	146.6 (2)	Os(3)–Os(4)–C(41)	114.0 (2)
Os(4)–Os(3)–C(32)	112.7 (2)	Os(3)–Os(4)–C(42)	96.7 (2)
Os(4)–Os(3)–C(33)	101.4 (3)	Os(3)–Os(4)–C(43)	148.2 (3)
	Carbon–Osmium–Carbon Angles		
C(31)–Os(3)–C(32)	92.5 (3)	C(41)–Os(4)–C(42)	98.4 (4)
C(31)–Os(3)–C(33)	96.9 (4)	C(41)–Os(4)–C(43)	94.8 (4)
C(32)–Os(3)–C(33)	96.3 (4)	C(42)–Os(4)–C(43)	92.0 (4)
	Metal–Carbon–Oxygen Angles		
Os(3)–C(31)–O(31)	179.0 (6)	Os(4)–C(41)–O(41)	175.4 (8)
Os(3)–C(32)–O(32)	177.7 (6)	Os(4)–C(42)–O(42)	174.9 (7)
Os(3)–C(33)–O(33)	177.8 (7)	Os(4)–C(43)–O(43)	176.4 (9)
Rh(1)–C(1)–O(1)	140.6 (5)	Rh(2)–C(1)–O(1)	133.0 (5)

[a] Intra-ring bond angles are provided in the supplementary material. [b] Esd's in parentheses.

At room temperature the ^{13}C NMR spectrum of IV consists of a triplet at δ 240.18 (J_{Rh-C} = 34 Hz) ppm assigned to the carbonyl which bridges the Rh edge of the cluster. A broad resonance at 180.67 ppm is assigned to the terminal carbonyls. At −90 °C the ^{13}C NMR spectrum is consistent with an asymmetric structure arising from the suggested positions of the hydrogens in the molecule, since the broad band assigned to terminal carbonyls is split into

(33) Churchill, M. R.; Hollander, F. J. *Inorg. Chem.* **1979**, *18*, 843.

six signals of equal intensity. (Chemical shifts are provided in the Experimental Section.)

Acknowledgment. We thank the National Science Foundation for support of this work through Grant CHE84-11630. We thank Mr. Steven L. Mullen and Professor Alan G. Marshall for FT/ICR mass spectra. NMR spectra were obtained at The Ohio State University Campus Chemical Instrument Center (funded in part by the National Science Foundation, Grant 79-10019).

Supplementary Material Available: Listings of anisotropic thermal parameters, intra-ring bond distances, and intra-ring bond angles (18 pages); listings of structure factor amplitudes (132 pages). Ordering information is given on any current masthead page.

Novel Anionic Rearrangements in Hexacarbonyldiiron Complexes of Chelating Organosulfur Ligands

Dietmar Seyferth,* Gary B. Womack, and Michael K. Gallagher

Department of Chemistry, Massachusetts Institute of Technology, Cambridge, Massachusetts 02139

Martin Cowie and Barry W. Hames

Department of Chemistry, University of Alberta, Edmonton, Alberta, Canada T6G 2G2

John P. Fackler, Jr., and A. M. Mazany

Department of Chemistry, Texas A&M University, College Station, Texas 77843

Received June 18, 1986

Bridging organosulfur chelate ligands of type $-SCHRS-$ (R = H, Ph), $-SCH_2CH_2S-$, $-S(CH_2)_3S-$, and $-SCH_2$-*o*-$C_6H_4CH_2S-$ in their $Fe_2(CO)_6$ complexes are deprotonated by lithium diisopropylamide. The resulting anion in the case of the $-SCH_2CH_2S-$ ligand undergoes β-elimination to produce (μ-LiS)(μ-$CH_2{=}CHS$)$Fe_2(CO)_6$, but the anions derived from the other ligands undergo an intramolecular rearrangement which involves nucleophilic attack by the carbanion at an iron atom with displacement of an electron pair onto one of the sulfur atoms. Addition of an organic halide then results in alkylation of a sulfur atom. In the case of (μ-SCH_2S)$Fe_2(CO)_6$ this sequence results in formation of an $Fe_2(CO)_6$ complex of an alkyl dithioformate, (HC(S)SR)$Fe_2(CO)_6$. Complexes of the latter type also can be deprotonated. A similar anionic rearrangement then results in formation of novel RR'S–CS–$[Fe(CO)_3]_2$ complexes after alkylation of the intermediate sulfur-centered anion with R'X. The structures of three products of such reactions were determined by X-ray crystallography. (μ-$CH_3C(O)CH_2SCHS$)$Fe_2(CO)_6$ (**10**) crystallizes in the space group $P\bar{1}$ (a = 10.296 (2) Å, b = 11.306 (2) Å, c = 6.617 (1) Å, α = 100.45 (1)°, β = 93.36 (1)°, γ = 103.38 (1)°, V = 732.9 Å^3, and Z = 2). On the basis of 2073 observations and 194 parameters varied the structure has converged at R = 0.042 and R_w = 0.055. (μ-$C_2H_5SCHC_6H_4CH_2S$)$Fe_2(CO)_6$ (**19**) crystallizes in $P2_1/n$ (a = 15.003 (2) Å, b = 7.530 (1) Å, c = 16.599 (2) Å, β = 92.11 (1)°, V = 1874.0 Å^3, and Z = 4) and has refined to R = 0.053 and R_w = 0.055 with 2004 observations and 223 parameters varied. (μ-SCS-$(CH_3)_2$)$Fe_2(CO)_6$ (**22**) crystallizes in $P\bar{1}$ (a = 9.586 (1) Å, b = 10.276 (1) Å, c = 7.601 (1) Å, α = 92.18 (1)°, β = 111.52 (1)°, γ = 86.94 (1)°, V = 695.3 Å^3, and Z = 2) and has refined to R = 0.029 and R_w = 0.039 with 2395 observations and 196 parameters varied.

Introduction

In our studies of the preparation and reactivity of hexacarbonyldiiron complexes containing bridging organosulfur ligands,[1] we had occasion to prepare the methylenedithio-bridged complex **1** (Scheme I).[2] This compound is an inorganic analogue of an organic dithiane, **3**. The latter class of compounds has H_2CS_2 protons which are relatively acidic due to the electronic effects of the two adjacent sulfur atoms and hence such compounds are easily deprotonated by strong bases. This provides the basis for

Scheme I

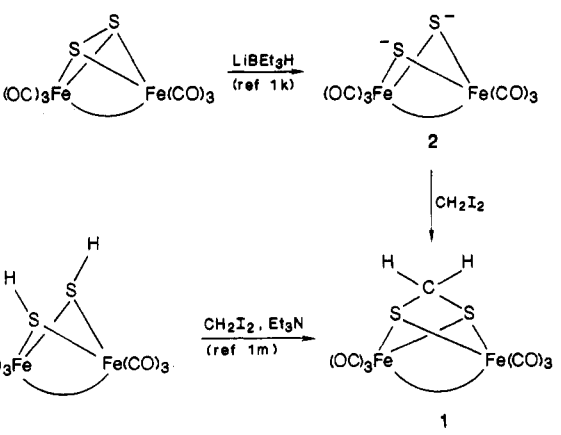

(1) (a) Seyferth, D.; Henderson, R. S.; Song, L.-C.; Womack, G. B. *J. Organomet. Chem.* **1985**, *292*, 9. (b) Seyferth, D.; Kiwan, A. M. *J. Organomet. Chem.* **1985**, *286*, 219. (c) Seyferth, D.; Kiwan, A. M.; Sinn, E. *J. Organomet. Chem.* **1985**, *218*, 111. (d) Seyferth, D.; Womack, G. B.; Dewan, J. C. *Organometallics* **1985**, *4*, 398. (e) Seyferth, D.; Womack, G. B.; Cowie, M.; Hames, B. W. *Organometallics* **1984**, *3*, 1981. (f) Mak, T. C. W.; Book, L.; Chieh, C.; Gallagher, M. K.; Song, L.-C.; Seyferth, D. *Inorg. Chim. Acta* **1983**, *73*, 159. (g) Seyferth, D.; Hames, B. W. *Inorg. Chim. Acta* **1983**, *77*, L1. (h) Seyferth, D.; Womack, G. B.; Song, L.-C. *Organometallics* **1983**, *2*, 776. (i) Seyferth, D.; Womack, G. B. *J. Am. Chem. Soc.* **1982**, *104*, 6839. (j) Chieh, C.; Seyferth, D.; Song, L.-C. *Organometallics* **1982**, *1*, 473. (k) Seyferth, D.; Henderson, R. S.; Song, L.-C. *Organometallics* **1982**, *1*, 125. (l) Seyferth, D.; Song, L.-C.; Henderson, R. C. *J. Am. Chem. Soc.* **1981**, *103*, 5103. (m) Seyferth, D.; Henderson, R. S. *J. Organomet. Chem.* **1981**, *218*, C34. (n) Seyferth, D.; Henderson, R. S.; Fackler, J. P., Jr.; Mazany, A. *J. Organomet. Chem.* **1981**, *213*, C21.

(2) (μ-SCH_2S)$Fe_2(CO)_6$ has been prepared earlier by the reaction of $Fe_2(CO)_9$ with 1,3-dithia-5-cycloheptene, and its structure has been determined by X-ray diffraction: Shaver, A.; Fitzpatrick, P. J.; Steliou, K.; Butler, I. S. *J. Am. Chem. Soc.* **1979**, *101*, 1313.

0276-7333/87/2306-0283$01.50/0